[American Journal of Science, Vol. 320, November, 2020, P. 790–814, DOI 10.2475/11.2020.02]

CONSTRAINTS ON SURFACE TEMPERATURE 3.4 BILLION YEARS AGO BASED ON TRIPLE OXYGEN ISOTOPES OF CHERTS FROM THE BARBERTON GREENSTONE BELT, SOUTH AFRICA, AND THE PROBLEM OF SAMPLE SELECTION

DONALD R. LOWE[*†], DANIEL E. IBARRA[*,**], NADJA DRABON[*], and C. PAGE CHAMBERLAIN[*]

ABSTRACT. Studies of Earth's surface temperature before 3.0 Ga have focused heavily on the oxygen isotopic composition of silica-rich sedimentary rocks called cherts. Interpretation of the results have suggested early surface temperatures ranging from as high as 70 ± 15 °C down to those that differ little from modern values. A major controversy centers on whether differences in the oxygen isotopic compositions of cherts over time reflect changing surface temperatures, changing ocean isotopic composition, or post-depositional diagenetic and metamorphic effects. We here present results of triple oxygen measurements of 3.472 Ga to 3.239 Ga cherts from the Barberton Greenstone Belt, South Africa. The best preserved samples based on geological evidence have $\Delta'^{17}O$ and $\delta'^{18}O$ values that plot generally on or near the equilibrium fractionation line for silica precipitated out of modern, ice-free sea water. Geologic considerations allow many potentially useful samples to be eliminated for paleotemperature analysis because of proximity to younger mafic intrusions or interactions with meteoric waters during deposition, both of which tend to lower preserved isotopic values. Our results of triple-O isotopic analyses of a suite of samples representing deposition under open marine, shallow shelf conditions suggest that Archean surface temperatures were well above those of the present day, perhaps as high as 66 to 76 °C. They demonstrate that geologic context, including depositional setting and post-depositional history, requires careful assessment before the significance of oxygen isotopic results can be evaluated.

INTRODUCTION

Geologic data relevant to estimating surface temperature on the Archean Earth derive in part from isotopic studies of 3.55 to 3.2 Ga silica-rich sedimentary rocks called chert. Made up largely of microquartz having a grain size <0.035 mm, chert forms layers from a few centimeters to over 400 m thick in Early Archean greenstone sequences in the Pilbara region of Western Australia and the Barberton Greenstone Belt (BGB), South Africa. Early Archean surface temperatures of 70±15 °C were estimated from studies of $\delta^{18}O$ of a wide variety BGB cherts by Knauth and Lowe (1978, 2003). However, using chert oxygen isotopes to interpret Archean surface temperature has proven controversial.

It has long been known that the oxygen isotopic composition of cherts shows a long-term secular $\delta^{18}O$ increase from maximum values of about 20 to 22 permil in the oldest, best preserved Archean chert to about 32 to 34 permil in modern marine chert (Perry, 1967; Knauth and Epstein, 1976; Perry and others, 1978; Knauth and Lowe, 1978; and many others). These secular changes have been interpreted to reflect either changes in the composition of sea water (Perry, 1967; Perry and others, 1978) or changes in the Earth's surface temperature (Knauth and Epstein, 1976; Knauth and Lowe, 1978, 2003). Additional complications arise because the oxygen isotopic composition of cherts can also be influenced by meteoric, diagenetic, hydrothermal, and

* Department of Geological Sciences, Stanford University, Stanford, California 94305, USA
** Department of Earth and Planetary Science, University of California, Berkeley, Berkeley, California
† Corresponding Author: drlowe@stanford.edu

metamorphic fluids active in their formation (Degens and Epstein, 1964; Becker and Clayton, 1976).

Controls on the $\delta^{18}O$ composition of sea water are complex, directly related to the relative contributions of low- and high-temperature alteration of crustal rocks (Muehlenbachs and Clayton, 1976; Muehlenbachs, 1998; Sengupta and Pack, 2018), and indirectly to tectonics and crustal dynamics, the abundance of continental crust, the nature of early weathering, and other still poorly constrained geologic processes that buffer seawater composition (Muehlenbachs, 1998; Jaffrés and others, 2007). Muehlenbachs and Clayton (1976) and Muehlenbachs (1998) modeled the oxygen isotopic composition of sea water as a balance between high temperature alteration of ocean floor basalts and low-temperature sea floor weathering. Sengupta and Pack (2018) and Sengupta and others (2020) emphasized the relative inputs from high temperature alteration of oceanic crust and low temperature continental weathering. They derived a trajectory of $\delta'^{18}O$ vs $\Delta'^{17}O$ sea water composition based on the ratio of low temperature versus high temperature alteration processes (Sengupta and Pack, 2018, their fig. 7). The results of these studies have suggested Archean oceans not substantially different in oxygen isotopic composition from modern sea water, although Sengupta and others (2020) emphasized that oceans with a higher $^{18}O/^{16}O$ ratio could be expected for an Archean world in which there were no large continents.

Direct tests of changing sea water composition using independent methods and measurements of igneous rocks likely to have interacted with seawater (for example, Drieberg and others, 2013; Zakharov and Bindeman, 2019; Peters and others, 2020) and the $\delta^{18}O$ of Archean carbonaceous matter (Tartese and others, 2017) have failed to reveal any evidence of major temporal changes in sea water oxygen isotopic composition. However, model results by a number of workers have suggested that ocean oxygen isotopic compositions may have varied over geologic time (Wallman, 2001; Pack and Herwartz, 2014). Johnson and Wing (2020) suggest that $\delta^{18}O$ of the Archean oceans may have been ~3.3 permil higher than present values. Hren and others (2009) report $\delta^{18}O$ and δD measurements for samples of the ~3.416 to 3.400 Ga Buck Reef Chert (BRC) in the Barberton Greenstone Belt, South Africa (fig. 1), and conclude that Archean surface temperatures were less than 40 °C. Sleep and Zahnle (2001), based on a model of carbon dioxide cycling on the Archean Earth, and Sleep and Hessler (2006), based on a model of Archean weathering of quartzose sediments of the Moodies Group in the BGB, conclude that temperatures on the early Earth could not have been hot. Kasting and others (2006) developed conceptual arguments as to why higher Archean temperatures are unlikely, and more recently Galili and others (2019) and Verard and Veizer (2019) have argued for more clement early climates and changing ocean water isotopic composition over time based on studies of marine iron oxides and tectonic models, respectively.

Many studies have emphasized the role of hydrothermal fluids in chert formation in the BGB (de Wit and others, 1982; Paris and others, 1985; Westall and others 2001, 2015; Hofmann, 2005; Hofmann and Bolhor, 2007), suggesting that Archean chert isotopic compositions directly reflect neither surface temperature or sea water composition. A recent study by Yanchilina and others (2019) has shown that Cenozoic deep-water biosiliceous oozes transform into quartz during burial at temperatures of about 60 °C, suggesting that the isotopic compositions of Archean cherts may be indicative of deep-burial diagenesis, not surface temperatures.

Levin and others (2014) were the first to study the triple-oxygen isotopic composition of Archean cherts and emphasized the potential of the method to resolve the roles of ocean composition, surface temperature, and other fluids in their formation. More recently, Liljestrand (ms, 2019), Liljestrand and others (2020), Sengupta and Pack (2018) and Sengupta and others (2020) have studied the triple oxygen isotopic

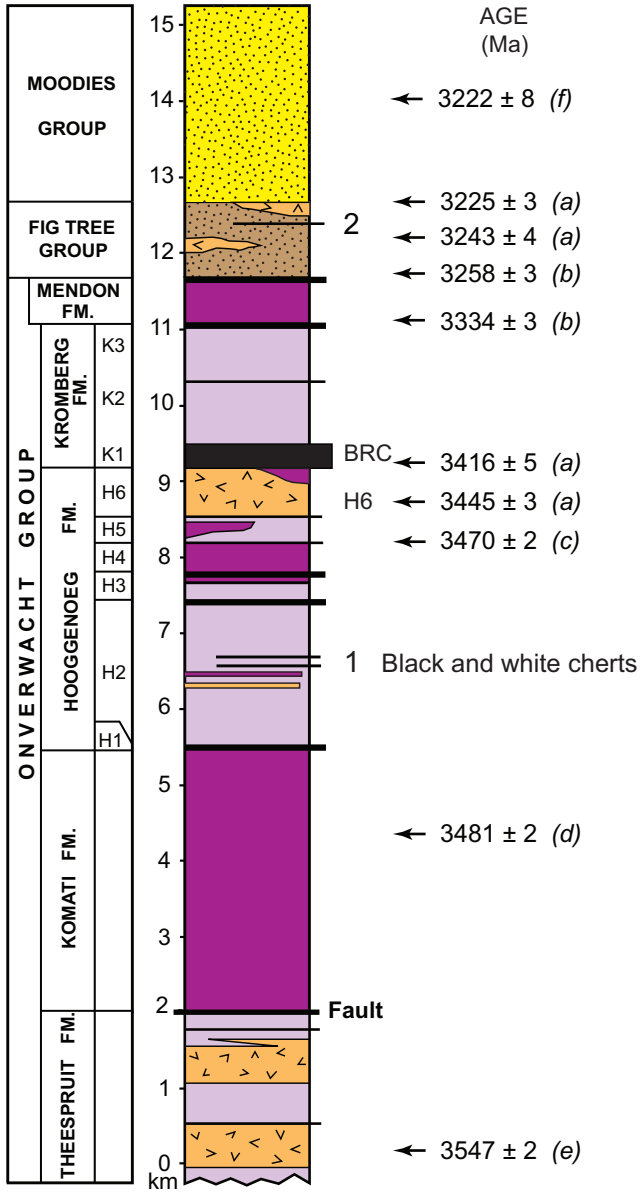

Fig. 1. Stratigraphic column of rocks in the Barberton Greenstone Belt, South Africa, showing key zircon ages and locations of the Buck Reef Chert (BRC) and sampled units in the lower Hooggenoeg Formation (1) and in the Fig Tree Group (2). Key: komatiitic volcanic rocks (purple), basaltic volcanic rocks (mauve), felsic volcanic rocks (orange), Fig Tree Group siliciclastic rocks (brown), and Moodies Group siliciclastic rocks (yellow). References for ages: (a) Kröner and others (1991); (b) Byerly and others (1996); (c) Byerly and others (2002); (d) Dann (2000); (e) Kröner and others, 1996; (f) Heubeck and others (2013).

composition of Proterozoic and Archean cherts, including many from the BGB, and suggest that present compositions reflect deposition at temperatures more like those prevailing today and diagenesis under the influence of meteoric waters of variable temperature. Blake and others (2010) concluded that Archean surface temperatures

were more like those of today based on the oxygen isotope studies of phosphate from the Barberton belt.

Clearly, early ocean oxygen isotopic composition and its role in influencing the composition of Archean cherts is an as yet unresolved issue. As a starting point for the present study, we accept the arguments of Muehlenbachs and Clayton (1976), Muehlenbachs (1998), and Sengupta and Pack (2018) and evidence provided from studies of the controls of sea water composition over time (for example Zakharov and Bindemen, 2019; Zakharov and others, 2019) that the oxygen isotopic composition of Archean sea water was basically similar to that of sea water today. While some recent studies have suggested that it is possible to model the oxygen isotope compositions of Archean cherts by a combination of meteoric and hydrothermal processes, we emphasize that there is little geologic evidence that these processes actually played any role in the composition of the Archean cherts studied here (Knauth and Lowe, 1978, 2003). In this study we apply triple oxygen isotope analysis combined with sedimentological and geological studies of 3.47 to 3.24 Ga cherts from the Barberton Greenstone Belt, South Africa, toward estimating the surface temperature of the Early Archean Earth. We emphasize that significant problems arise in interpreting the oxygen isotopic composition of Archean cherts without full consideration of their geologic and depositional context. Based on geologic and isotopic arguments we suggest that the best preserved BGB cherts indicate relatively high Early Archean surface temperatures.

GEOLOGIC SETTING OF SAMPLES

Samples analyzed in this study are from the Barberton Greenstone Belt (BGB), South Africa, and vary from about 3.472 to 3.239 Ga (fig. 1). Most are from the 200 to 400 m thick Buck Reef Chert (BRC), ~3.4 Ga, in the upper part of the 10 to 12 km thick section of mafic and ultramafic volcanic rocks of Onverwacht Group (figs. 1 and 2). The BRC was deposited on a subsiding felsic volcanic platform represented by the underlying member H6 of the Hooggenoeg Formation (figs. 1 and 2). H6 is the volcanic expression of a regional episode of felsic igneous activity marked at depth by TTG (tonalite-trondhjemite-granodiorite) intrusions exposed today around southern edge of the BGB. Underlying H6 is thick succession of mafic and komatiitic volcanic rocks (figs. 1 and 2B) with thin intervening silicified cherty sedimentary units marking intervals of volcanic quiescence (Viljoen and Viljoen, 1969; Lowe and Byerly, 1999). Coincident with the magmatic events of H6, these underlying rocks were flushed by voluminous hydrothermal and metamorphic fluids, the cherty sedimentary layers were recrystallized into fine, sugary mosaics of quartz, and their $\delta^{18}O$ compositions were reset to lighter values, most 10 to 16 permil (Knauth and Lowe, 1978, 2003).

As H6 magmatic activity waned, the subaerial volcanic surface was eroded and eventually subsided below sea level. Volcaniclastic sediments eroded from the felsic complex and interbedded evaporites accumulated in small extensional basins and as a flanking alluvial and shallow-marine fringe (Lowe and Fisher-Worrell, 1999; Tice and Lowe, 2006). The lower part of the overlying marine facies of the BRC is composed of 100 to 200 m of black and white banded chert (Tice and Lowe, 2006) that consists of alternating bands from <1 to about 10 cm thick of dark gray to black carbonaceous chert and white-weathering, translucent chert, both composed largely of microcrystalline quartz (fig. 3). The black bands contain current-worked carbonaceous particles and mat-like carbonaceous laminations representing early biogenic sediments (Tice and Lowe, 2006). The lower BRC shows a rich array of features indicating deposition of siliceous particles, silica precipitates, and biogenic sediments on a subsiding, weakly current active, storm-influenced marine platform (Tice, ms, 2005; Tice and Lowe, 2006). Continued subsidence of the depositional

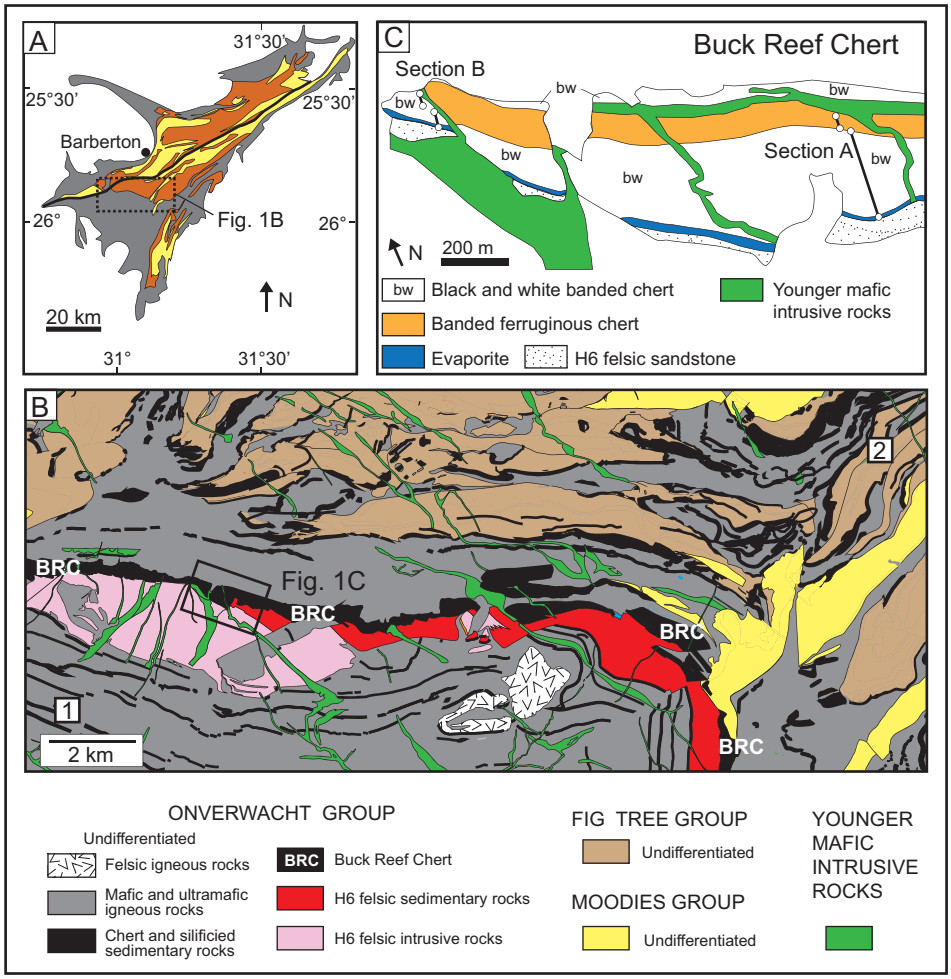

Fig. 2. Geology of the Barberton Greenstone Belt. (A) Generalized geologic map of the Barberton Belt showing the areal distribution of the major stratigraphic divisions: Onverwacht Group (gray), Fig Tree Group (brown), and Moodies Group (yellow). (B) Geologic map of the south central part of the Barberton Belt showing the locations of the samples collected and discussed in this study. Modified from Lowe and others (2012). BRC indicates the outcrop of the Buck Reef Chert. Numbers 1 and 2 show locations of samples analyzed from the Hooggenoeg Formation and Fig Tree Group, respectively. Location of figure C shown. (C) Details of the study area of Tice (ms, 2005) showing the locations of his section "A", from which most samples of the Buck Reef Chert were collected for this study, and section "B", which is surrounded closely by bodies of intrusive mafic igneous rock that may have reset oxygen isotopic values of nearby cherts.

surface into progressively deeper-water saw the accumulation of increasingly iron-rich banded cherts in environments of decreasing current, wave, and storm activity (Tice and Lowe, 2006). Above 120 m above the base of the BRC, the dark bands become slightly ferruginous and above about 180 m the rock is banded ferruginous chert (BFC). Where fresh, BFC includes dark bands composed of intergrown siderite, microquartz, and carbonaceous matter and light bands of nearly pure microquartz. In virtually all surface exposures, the siderite has been oxidized to hematite or goethite and the carbonaceous matter has been oxidized by modern weathering (Lowe and Byerly, 2007).

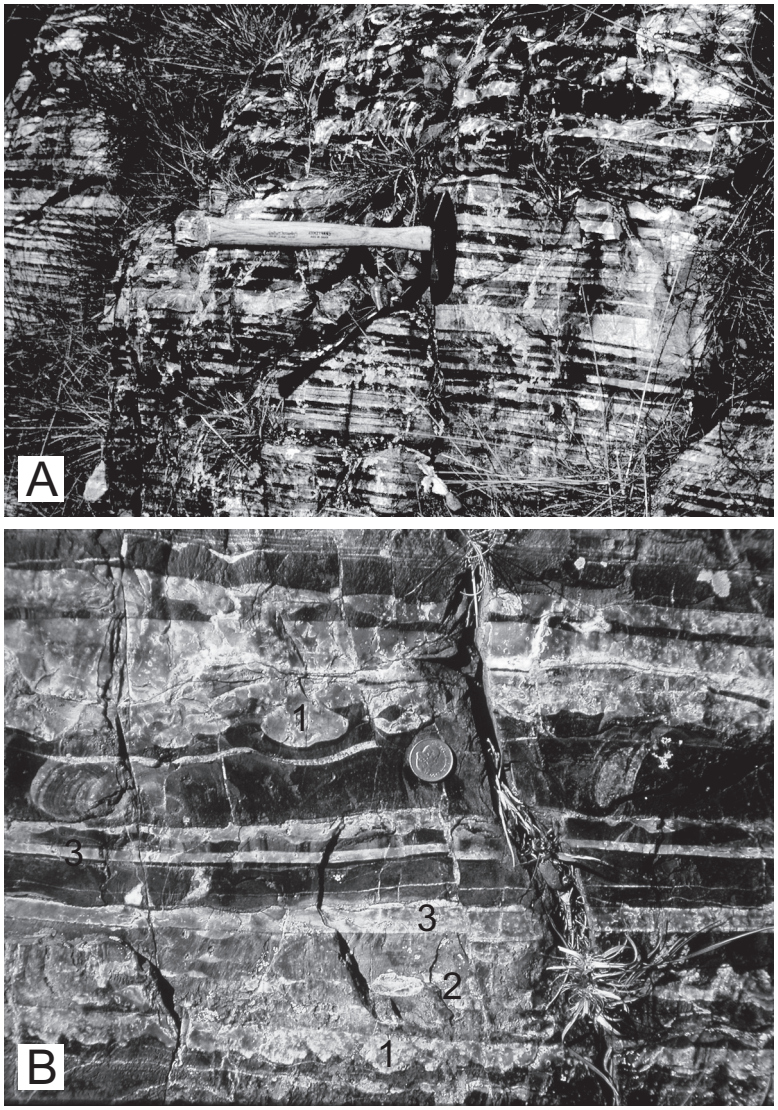

Fig. 3. Outcrops of the black and white banded chert of the Buck Reef Chert. (A) Relatively evenly and uniformly banded black and white chert. (B) Banded chert showing effects of early soft-sediment deformation, including loading of the still-soft, white-chert-band sediments into the underlying, soft, black carbonaceous sediments (1) and boudinage and deformation of some individual, soft white chert bands (2). At the same time, most white bands remain undisrupted (3), indicating that this deformation does not reflect large-scale, late-stage events.

BRC samples for the present study were collected from surface outcrops of the lower part of the BRC, including a number from section "A" of Tice (Tice, ms, 2005; Tice and Lowe, 2006) (fig. 2C), and represent mainly the white, carbon-free bands. This section was also the source of samples for the study of Hren and others (2009). Two other samples, SAF-131 and SAF-160, are from the main zone black and white banded chert in nearby BRC sections. There are problems with samples from the lowest 10 m and above about 100 m in section "A" of Tice (ms, 2005) because these parts of the section include a number of post-BRC mafic dikes and

sills that have had visible effects on chert texture and which appear, based on our own studies, to have reset the nearby chert to lower $\delta^{18}O$ values. No samples were included from section "B" of Tice (ms, 2005) because of its proximity to large mafic intrusions (fig. 2C). One sample, SAF-475-2, is from section "A" at 135 m. One chert sample (SAF-135) was collected from the basal evaporite member of the BRC, which accumulated in coastal brine ponds developed around and upon the alluvial fringe on the subsiding H6 volcanic complex. In addition, two samples (SAF-52, loc. 1 in fig. 1) were collected from 5 to 10-m-thick units of black and white banded chert in the lower Hooggenoeg Formation, more than 2000 m below the BRC (fig. 1), where $\delta^{18}O$ has been lowered during the regional H6 igneous and metamorphic event (Lowe and Knauth, 1978, 2003). A single sample of translucent Fig Tree chert (SAF-73) representing sediments deposited on the flanks of a small fan delta (Lowe and Nocita, 1999; Drabon and others, 2019) was included for comparison (loc. 2 in fig. 1).

METHODOLOGY

Chert samples were measured by laser fluorination at Stanford University using a Thermo 253 Plus 10kV IRMS following previously established methods (Sharp, 1990; Hren and others, 2009; Mix and others, 2016; Sharp and others, 2016). Samples were not crushed or pre-treated. Chips from the chert samples were exposed to BrF_5 and heated using a CO_2 infrared laser in a vacuumed fluorination line. Laser times were less than 5 minutes for all samples (after Sharp, 1990) and samples were pre-fluorinated for 2 hours to 2 days to remove all absorbed water vapor. Following fluorination the evolved O_2 gas was frozen onto a 5Å mol sieve under liquid nitrogen and then transferred by He through a 5Å mol sieve column to remove NF_3 and other contaminants. The final purified O_2 aliquot was equilibrated with the 253 Plus bellows for 6 minutes to ensure quantitative release of the sample into the mass spectrometer. All steps in the laser fluorination line are timed to ensure consistency and conducted by a single user. Measurements were made for 1.5 to 3+ hours at 5V on mass $^{32}O_2$ and corrected using a pressure baseline correction following Yeung and others (2018) that was calibrated periodically (bi-weekly to monthly). In-house and previously measured standards show long-term external reproducibility of our hydrothermal quartz standard, NM-Q (n = 47 measurements over 10 months), of 0.137 permil for $\delta'^{18}O$ and 0.011 permil for $\Delta'^{17}O$ for the sessions in 2018 and 2019 in which samples from this study were analyzed. Analyses are reported relative to session averages of previously published high-precision SCO (n = 23), UWG-2 (n = 16), and NM-Q (n = 47) values (Pack and Herwartz, 2014; Sharp and others, 2016; Wostbrock and others, 2018, 2020) analyzed during each analytical period (see table 1 and Appendix table A1 for details).

RESULTS

The results of the present study are shown in table 1, Appendix table A1, and in a $\Delta'^{17}O$ vs $\delta'^{18}O$ plot in figures 4A, 4B. The definitions of these terms and the sea water-silica equilibrium fractionation curve (fig. 4) are from Sharp and others (2016). The re-calibration by Wostbrock and others (2018) of sea water-silica fractionation is within error of the original calibration by Sharp and others (2016). Following the reasoning of Muehlenbachs and Clayton (1976), Muehlenbachs (1998), and Sengupta and Pack (2018), we conclude the composition of sea water has not changed significantly over geologic time and is plotted (fig. 4) as being approximately that of modern ice-free sea water (Sengupta and Pack, 2018).

TABLE 1

Triple oxygen isotope data of samples from the Barberton Greenstone Belt, South Africa. See supplemental table for details on standards and replicates

Sample ID	Sample Type	Formation	Age (Ga)	$\delta^{18}O$ (VSMOW)	$\delta'^{17}O$ (VSMOW)	$\delta'^{18}O$ (VSMOW)	$\Delta'^{17}O$ (λ=0.528)
TSA5-5	White/Translucent Chert	BRC, Kromberg Fm.	~ 3400	20.182	10.479	19.980	-0.070
TSA5-7	White/Translucent Chert	BRC, Kromberg Fm.	~ 3400	18.468	9.622	18.299	-0.040
TSA5-8	White/Translucent Chert	BRC, Kromberg Fm.	~ 3400	18.658	9.662	18.486	-0.098
TSA5-10	White/Translucent Chert	BRC, Kromberg Fm.	~ 3400	18.152	9.453	17.989	-0.045
TSA5-30	White/Translucent Chert	BRC, Kromberg Fm.	~ 3400	19.964	10.399	19.767	-0.038
TSA5-22	Black Chert	BRC, Kromberg Fm.	~ 3400	20.068	10.411	19.869	-0.080
SAF-52-8	White/Translucent Chert	lower Hooggenoeg Fm.	~ 3472	14.670	7.648	14.563	-0.041
SAF-52-13	White/Translucent Chert	lower Hooggenoeg Fm.	~ 3472	15.171	7.898	15.057	-0.052
SAF-73-7	White/Translucent Chert	Mapape Fm., Fig Tree Group	~ 3240	17.569	9.162	17.416	-0.034
SAF-131-11	White/Translucent Chert	BRC, Kromberg Fm.	~ 3400	19.284	10.027	19.100	-0.058
SAF-131-12	White/Translucent Chert	BRC, Kromberg Fm.	~ 3400	19.976	10.385	19.779	-0.059
SAF-135-4	White/Translucent Chert	upper Hooggenoeg Fm.	~ 3420	16.075	8.381	15.947	-0.039
SAF-160-4	Black Chert	BRC, Kromberg Fm.	~ 3400	20.881	10.846	20.666	-0.065
SAF-475-2	White/Translucent Chert	BRC, Kromberg Fm.	~ 3400	15.992	8.341	15.865	-0.036

Two main isotopic groups of samples can be distinguished in the present study (figs. 4A, 4B). Group 1 includes samples from the main body of the black and white banded BRC and the one Fig Tree sample. These rocks show $\delta'^{18}O$ values between +17.57‰ and +20.88‰ and $\Delta'^{17}O$ from −0.081‰ to −0.034‰. We regard these 8 samples and 1 from Hayles and others (2019) as being the least contaminated and least altered samples of the suite. Environmental analysis of Tice and Lowe (2006) indicate that they most likely represent silica initially precipitated under open marine, shallow shelf conditions that has not been discernably affected by later igneous activity or contaminated during deposition by siliciclastic materials.

Group 2 samples show significantly lower $\delta'^{18}O$, from +14.67 to +16.08‰, but $\Delta'^{17}O$ comparable to those of Group 1. This group includes the samples from lower in the Hooggenoeg Formation, about 3.472 Ga, that have been thermally upgraded to sugary quartz and at least partially equilibrated with surrounding mafic volcanic rocks under fluid-rich metamorphic conditions at about 3.45 Ga (Knauth and Lowe, 1978, 2003), and the sample from the evaporitic member of the BRC, which was deposited at about 3.416 Ga in evaporitic brine ponds under the influenced of freshwater runoff from surrounding land areas and evaporitically concentrated sea water (Lowe and

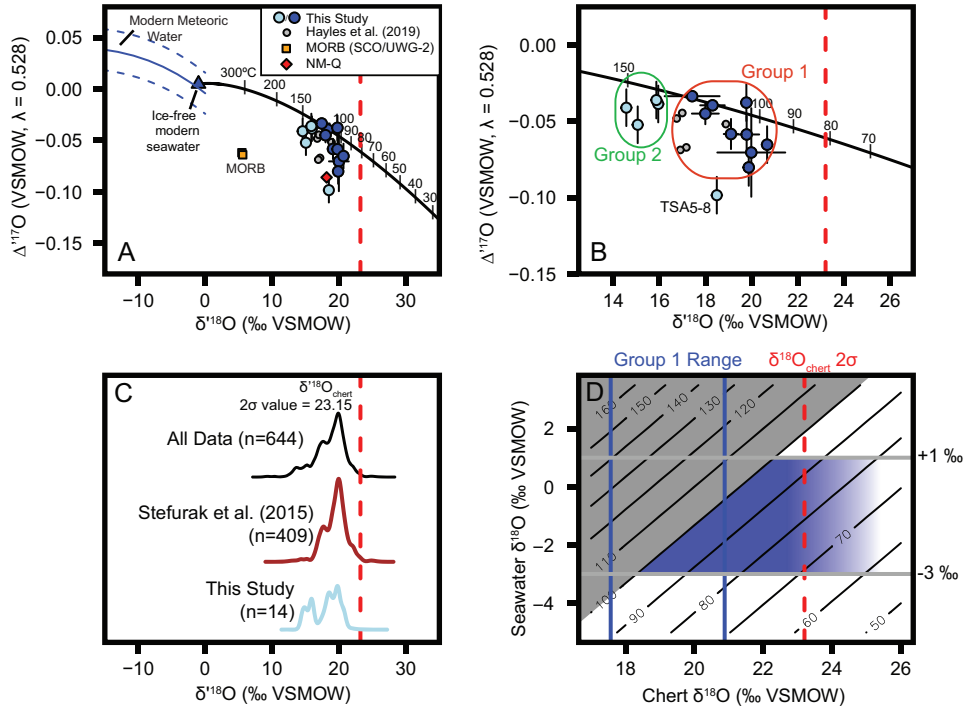

Fig. 4. Oxygen isotope measurements of cherts in the Barberton Greenstone Belt. (A) Triple oxygen isotope plot ($\Delta'^{17}O$ vs $\delta'^{18}O$) of data from this study and previous published data from Hayles and others (2019) with silica-water fractionation curve (black) based on Sharp and others (2016) with the ice-free sea water value (blue triangle) from Sengupta and others (2018). Methods described in the text. All error bars are 1σ. Orange squares are approximate MORB values (based on SCO and UWG-2), red diamond is the NM-Q hydrothermal quartz standard, and the blue lines show the modern meteoric water field from Sengupta and others (2020). (B) Details of plot in A with Group 1 and Group 2 samples identified as discussed in the text. (C) Kernel smoothed histogram of published oxygen isotope measurements (converted to linearized $\delta'^{18}O$ values) from references listed in the text. Red vertical line on all diagrams is the 2σ value of all data in C. (D) Solution space of temperature (contours in °C) for chert $\delta^{18}O$ versus seawater $\delta^{18}O$. Gray region is greater than 100 °C and blue region is plausible solution space for seawater from +1 to −3 ‰.

Fisher-Worrell, 1999). There is also one sample from the BRC at 135 m in Tice's section "A" that we suspect has been affected by nearby mafic intrusions. All Group 2 samples have identifiable depositional settings where meteoric water played a role in sedimentation or they have been affected by post-depositional hydrothermal and/or metamorphic alteration.

Another sample (TSA5-8) is from the main body of the BRC and shows a $\delta'^{18}O$ consistent with those of the freshest cherts but has low value of $\Delta'^{17}O$ (−0.098). The origin of this low $\Delta'^{17}O$ value is unclear although proximity to a small mafic intrusion is possible.

All available $\delta^{18}O$ values of cherts from the Onverwacht Group not representing silicified volcanic rocks, carbonates (Cammack and others, 2018), volcaniclastic materials, or siliciclastic sediments and where there is some control on conditions of deposition were compiled for comparison with the results obtained here (fig. 4C), including those of Knauth and Lowe (1978, 2003), Katrinak (ms, 1987), Hren and others (2009), Stefurak and others (2015b), and Hayles and others (2019).

DISCUSSION

Archean Surface Temperature

Our analysis suggests that Group 1 cherts provide the best constraints on the temperature of the Archean surface environment. If the $\delta'^{18}O$ values of Group 1 cherts represent the freshest, least altered samples, most fall on or just to the left of the equilibrium fractionation curve of Sharp and others (2018) that passes near the composition of present day ice-free ocean water (fig. 4A), for which $\delta'^{18}O = -1‰$, $\Delta'^{17}O = 0.004‰$. The $\delta'^{18}O$ data from Group 1 samples are centered on a formation temperature of about 80 to 120°C (figs. 4B, 4C).

At least 3 considerations suggest that some modification of these temperature estimates is needed: (1) Knauth and Lowe (1978, 2003), who measured a maximum $\delta^{18}O$ of about 22 permil on BRB cherts, suggested that the highest $\delta^{18}O$ value probably represents the least altered chert since virtually all post-depositional alteration tends to lower $\delta^{18}O$ values. Most diagenetic reactions, hydrothermal activity, and metamorphism will shift the oxygen isotopic composition of chert to lower $\delta^{18}O$ values (Knauth and Lowe, 1978, 2003; Marin and others, 2010; Stefurak and others, 2015b; Hayles and others, 2019). The highest $\delta'^{18}O$ value measured in this study is about 21 permil (SAF-160-4) corresponding to a temperature of about 96 °C (fig. 4A). However, considering the entire compiled data set of $\delta^{18}O$ values (fig. 4C), the upper 2σ for the total spread of $\delta^{18}O$ values is about 23 permil corresponding to a surface temperature of about 82 to 83 °C. This is very close to highest Barberton Belt chert isotopic composition of $\delta^{18}O = 23.39‰$ reported by Stefurak and others (2015b) from the Mendon Formation and to the maximum $\delta^{18}O$ for microquartz in the ~3.45 Ga Strelley Pool Chert in Western Australia of ~22 permil by SIMS (Cammack and others, 2018). These data provide remarkably consistent values for the maximum $\delta^{18}O$ in microquartz from Early Archean cherts and for the resulting Early Archean paleotemperature estimates based on them.

(2) As noted by Knauth and Lowe (1978), it also seems likely that we have not yet discovered the highest preserved $\delta^{18}O$ values in Archean cherts. Examining the many $\delta^{18}O$ and $\delta'^{18}O$ values of microquartz available for >3.0 Ga cherts in Barberton and the Pilbara regions, the maximum values show a remarkable convergence at about 22 to 23 permil, as noted above. This convergence suggests to us that the true maximum preserved value is probably not significantly greater: in other words, future, more exhaustive bulk rock and microanalytical analyses will probably not yield $\delta^{18}O$ values significantly larger than these. However, allowing that chert enclaves showing slightly higher values might exist, we suggest that the maximum preserved $\delta'^{18}O$ value might be about 24 permil, only about 0.5 permil higher than values determined by SIMS analysis (Stefurak and others, 2015b).

(3) While we have sought to eliminate all veins and patches of late, post-depositional quartz from our analyses, all cherts in the BGB are cut by a network of very fine quartz veins that truncate layering (fig. 5) and are filled by relatively coarse-grained quartz (fig. 5B). Figures 2A, 2B, and 2C of Sengupta and others (2020) show samples of Archean cherts that they measured criss-crossed by a complex network of small veins filled with coarser quartz. Although Stefurak and others (2015b) showed that some quartz veins have $\delta^{18}O$ values little different from those of the surrounding chert, many others are of hydrothermal origin and have significantly lower $\delta^{18}O$ values (Knauth and Lowe, 2003). These veins cannot be separated from the surrounding microquartz matrix and some were inevitably included in the bulk rock analyses. The effect of hydrothermal veins, which commonly have $\delta^{18}O$ values in the range of 10 to 15 permil (for example, Kerrich and Fryer, 1979), consistent with the values of quartz veins and recrystallized cherts lower in the Barberton sequence (Knauth and Lowe,

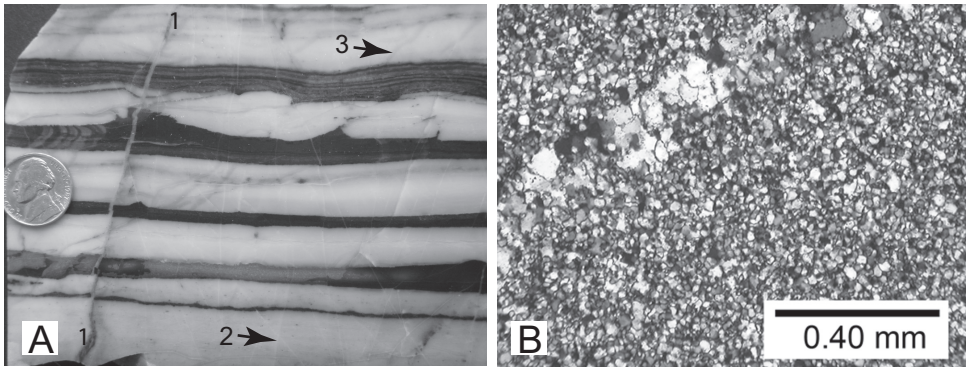

Fig. 5. Hydrothermal quartz veins in the Buck Reef Chert. (A) Typical banded chert showing a relatively large quartz vein (1, left side). These larger veins were eliminated from all samples analyzed. Very fine veins, such as those present at 2 and 3, could not be avoided and were present in all samples. (B) Example of one of the sub-millimeter wide hydrothermal quartz veins (upper left) cutting microcrystalline quartz of the Buck Reef Chert.

1978, 2003), would be to lower the measured $\delta'^{18}O$, perhaps by 1 to 2 permil, depending on their abundance and overall vein isotopic compositions.

Based on the 2σ spread of measured Buck Reef Chert compositions in this study and the highest $\delta^{18}O$ reported by Stefurak and others (2015b), the highest $\delta'^{18}O$ of microquartz in the BRC chert is probably about 23 permil corresponding to a surface temperature of about 82 to 83 °C. If we minimally account for the effects of possible still undiscovered enclaves with slightly higher $\delta^{18}O$ values and of the effects of hydrothermal veins on bulk analyses, we estimate the maximum $\delta'^{18}O$ of these rocks as 24 to 26 permil corresponding to temperatures of about 76° to 66 °C, respectively, for a sea water value of −1 permil (fig. 4). Based on the present results and considering all available O-isotopic analyses of Archean cherts for which we have some control on geologic setting and depositional conditions and which appear to represent open marine deposits, this represents our best estimate of the surface temperature 3.42 to 3.25 Ga. The total solution space for the present results is shown in figure 4D.

Other Archean Surface-Temperature Estimates

Hren and others (2009) presented the results of combined deuterium and oxygen isotopic analyses of BRC samples from the same section "A" (fig. 2) studied by Tice (Tice, ms, 2005; Tice and Lowe, 2006) and from which many of the samples in this study were collected. They concluded that the Archean oceans were isotopically depleted, in the range of −18 to −8 permil, compared to modern oceans and that Archean surface temperatures were ≤ 40 °C. However, Knauth (ms, 1973) experimentally determined that hydrogen in cherts was stable only at temperatures less than about 200 °C. At higher temperatures, the structurally bonded OH^- groups that represent the potential primary source of Archean hydrogen in cherts is exchanged with surrounding fluids. All of the rocks in the BRC have experienced temperatures above 300°C, perhaps for long periods of time (Xie and others, 1997; Tice and others, 2004). There is no reason to expect that they would have retained any primary Archean hydrogen or surface water.

Blake and others (2010) report oxygen isotopic analyses of phosphates from the Barberton Belt. Based on the analytical results, they divided their samples into two groups: group 1 with relatively low $\delta^{18}O_P$ values, 11.2‰ to 9.3‰ (3 samples), and group 2 with relatively high $\delta^{18}O_P$ values, 16.2‰ to 19.9‰ (7 samples). One sample

had an intermediate $\delta^{18}O_P$ of 13.8 permil. Paleotemperatures were calculated from the higher $\delta^{18}O_P$ values of group 2 samples, assuming equilibrium with sea water with $\delta^{18}O_P = 0\%$. The calculated paleotemperatures ranged from 26°C to 35°C, consistent with an essentially modern temperature for the Archean surface.

However, as noted by Blake and others (2010) all but one of the group 2 samples contained abundant iron, mainly in the form of the iron oxides hematite and goethite but also with traces of iron carbonates. As reported by Blake and others (2010) there was an absence of apatite in these samples: all of the phosphate was included within the iron phase, not as separate phosphate minerals. The Fe_2O_3 contents of group 2 samples ranged from as low of 0.54 percent for a sample of laminated tuff to as high as and 16.89 and 49.9 percent, averaging about 16.35 percent for the 6 non-tuffaceous samples. A major problem with this sample set was that all rocks were collected from surface exposures. Banded ferruginous chert and most of the Barberton banded iron formation, which represent the main lithologies sampled by Blake and others (2010), contain abundant siderite as a major iron-bearing mineral when seen in core from the subsurface. Virtually all samples of these lithologies that we have studied from surface environments show hematite and goethite as weathering products after siderite. We would conclude that these analyses and the inferred paleotemperature results are problematic because most of the iron oxides in these samples probably formed through Quaternary weathering, mainly of siderite that is present in rocks below the modern weathering zone. One particularly problematic sample of Blake and others (2010), AL03-28I, the sample with the highest δ18OP = 19.9‰, came from surface outcrops of the Buck Reef Chert. This locality is noteworthy because it includes chert-ironstone bodies formed by Quaternary weathering of the uppermost Buck Reef Chert (Lowe and Byerly, 2007). The iron oxide formed during deep (up to >100 meters) Quaternary leaching and weathering of sideritic banded ferruginous chert that is present at depth as seen in ICDP core No. BARB3 taken nearby in 2012. Also, the observation by Blake and others (2010) that the two most abundant iron oxides in their samples are hematite and goethite is noteworthy because goethite is thermally unstable, essentially unknown as sedimentary material in pre-Phanerozoic rocks (Yapp, 2001), and, in these rocks, almost certainly originated by Quaternary weathering (Lowe and Byerly, 2007).

A number of recent papers have used microanalytical tools, SIMS and microprobe, to study the small-scale isotopic heterogeneity of Archean cherts. Marin-Carbonne and others (2011, 2012) report on the oxygen and silicon isotopic analysis of cherts using ion microprobe techniques for spot analyses. Their results confirm the heterogeneity of the samples studied and the complex histories of silicification experienced by such ancient chert samples. However, the sample suite, including one from the Barberton Belt, was from museum specimens collected by others. The sample from the Barberton Belt was a chert from either the Mendon Formation or the Weltevreden Formation collected by Preston Cloud from the Sheba gold mine along the northern edge of the Belt. Because this and most of their samples could not be independently constrained in terms of depositional conditions and depositional and early diagenetic fluids, we would not want to use them to estimate the composition of Archean sea water.

Stefurak and others (2015b) examined Si and O isotopic variations in different textural generations of cherts in the Barberton Belt, especially cherts of the Mendon Formation at the top of the Onverwacht Group (fig. 1), using wavelength-dispersive spectroscopy and SIMS. Their studies showed widespread, spatial variations in O and Si isotopes at the sub-millimeter scale, some correlated with textural types of chert. They noted that the highest $\delta^{18}O$ value encountered was 23.39 permil and that the $\delta^{18}O$ of coarse cavity-fill quartz tends to decrease from higher values in the finer-

grained quartz around the outsides of the cavities to lower values in the coarse-grained fill at the centers of the cavities.

Cammack and others (2018) using SIMS studied the Si and O isotopic composition of cherts from the Early Archean Strelley Pool Chert in the Pilbara of Western Australia (Lowe, 1983; Allwood and others, 2006). Their study, like other studies of small scale variability of Si and O isotopes in these ancient cherts, emphasizes the spatial heterogeneity of chert isotopic compositions and silicification histories. They conclude that, "None of the SPF [Strelley Pool Formation] quartz examined is interpreted to have formed as a direct precipitate from Paleoarchean seawater." This is consistent with our results that all of the BRC microquartz formed by early diagenetic alteration of pre-existing, less ordered siliceous sediments. We would note four significant points made by this paper: (1) the spatial microheterogeneity of the Si and O isotopic compositions; (2) "microquartz is the earliest textural generation of quartz and has a maximum $\delta^{18}O$ (Qz) of ~22 **permil** by SIMS;" (3) Higher $\delta^{18}O$ values reported by Cammack and others (2018) are from coarser generations of quartz with the highest values from coarse megaquartz interpreted to have formed during post-Archean weathering; and (4) Crosscutting megaquartz veins show $\delta^{18}O$ between 16 permil and 19 permil.

Hayles and others (2019) also report on triple oxygen isotope studies of cherts from the Barberton belt, including samples from the BRC and from the 3.223 to 3.215 Ga Moodies Group. Their reported results are included in figures 4A and 4B. The Onverwacht Group samples are reportedly from the BRC section "B" (fig. 2C) of Tice (Tice, ms, 2005) (Hayles, Personal Communication, 2019). Given that these samples are from section "B", the values are likely to have been reset because section B is surrounded within 50 m by a number of large diabase bodies and may have experienced isotopic resetting (fig. 2C; Lowe and others, 2012). Additionally, their samples from the Moodies Group show $\delta'^{18}O$ values that are quite low, $\delta'^{18}O < 15‰$. These samples are from thin chert layers associated with microbial mats (Homann and others, 2015) within intertidal to supratidal sequences and may have formed in part under the influence of meteoric waters under shallow subaqueous to subaerial conditions (Heubeck, 2009; Gamper and others, 2012) or diagenetically by the replacement of primary carbonate deposited in gas-filled cavities (Homann and others, 2015). Their isotopically low values almost certainly reflect the influence of meteoric water during diagenesis rather than their formation from an isotopically light Archean ocean.

Yanchilina and others (2019) studied the transformation of Cenozoic opaline biosiliceous oozes in the deep Pacific Ocean into opal-CT and finally into quartz with burial. Their study showed that the transition to quartz occurred at burial temperatures on the order of 60 °C at 400 to 500 m below the sea floor. They conclude that, "Without knowing porewater $\delta^{18}O$ and temperature in which these cherts precipitated, it is impossible to draw conclusions about temperature of the Archean ocean." Knauth (1992) also observed, "Studies have repeatedly shown that [deep water] siliceous oozes are initially laid down as biogenic opal-A and are then transformed during burial to Opal-CT and then quartz. The bedded chert produced in this way is composed of quartz formed during deep burial at temperatures of up to 80 degrees C, or higher. It can take more than 60 million years for the ooze to completely convert to quartz. Isotopic analyses of these types of chert yield information mainly about late diagenesis; determination of paleoclimatic temperatures is not possible unless it can be independently demonstrated that the transformation from opal to quartz occurred during shallow burial." These results are also consistent with those of Kolodny and Epstein (1976) who showed that the isotopic composition of deep sea cherts may not be frozen in until several millions of years after deposition and after considerable

burial. These and many other studies show that deep water siliceous sediments that have undergone conversion to quartz during deep burial may provide paleotemperature and fluid compositional details relevant to their burial history, but not on the conditions of deposition or the surface temperature. Hence our emphasis for Archean paleotemperature analysis on cherts representing sediments deposited under shallow marine conditions and converted to microquartz at shallow burial depths.

Liljestrand (ms, 2019) and Liljestrand and others (2020) have recently studied Proterozoic and Archean cherts with, among other goals, an aim of exploring the relevance of oxygen isotopes toward interpreting ancient surface temperatures. These studies conclude that the chert isotopic record is best described as a product of alteration with higher-temperature, meteoric-derived groundwater and that "neither changes in seawater temperature nor changes in seawater O-isotope composition are required." Their studies focused on two groups of cherts: (i) nodular Proterozoic cherts in sequences deposited in shallow-water to intertidal conditions, and (ii) cherts in Proterozoic and Archean iron formation. The origin of nodular cherts in carbonate sequences has been addressed by Knauth (1979) and McBride and others (1999), who have concluded that most formed under conditions involving the mixing of meteoric and marine waters. These cherts would be unsuitable for estimating ancient paleotemperatures where strictly open marine waters are assumed. Virtually all Archean iron formation was deposited in deep, quiet water and was probably deposited much like modern deep-water biosiliceous oozes, except for having not included biogenic silica. Their diagenesis and conversion to a quartz-rich rock may have closely followed paths like that of modern deep water siliceous oozes (for example, Yanchilina and others, 2019). Lowe (1999) observed that cherts deposited in deeper water in the Barberton Greenstone Belt show evidence of lithification after significant burial and compaction. These cherts probably formed under conditions differing substantially from those at the surface and would not have been suitable cherts for surface temperature analysis (Knauth, 1992; Yanchilina and others, 2019). No nodular cherts or cherts from iron formations or from Archean deep-water facies were included in the present study.

Sengupta and others (2020) present a detailed analysis and discussion of the triple oxygen isotopic composition of chert samples from the Barberton and Pilbara belts, as well as younger samples, concluding that they do not support interpretations of a hot early surface environment. We would agree. Most of the samples, although located precisely, are essentially unconstrained in terms of local geological setting and conditions of sedimentation and metamorphism, most represent black chert units rather than white chert bands and therefore may have been lithified and converted to quartz substantially after deposition, and all have relatively low $\delta^{18}O$ values, as low as 13.67 permil for one sample from the metamorphosed and isotopically reset units below the H6 volcanic unit in the Onverwacht Group. The thin section photomicrographs of Archean cherts shown by Sengupta and others (2020, their figs. 2A, 2B, and 2C) show samples are cut extensively by veinlets of later, coarser probably hydrothermal quartz. While these samples may reveal significant information about post-depositional events, including hydrothermal activity and metamorphism, they are not, without further studies, useful for surface paleotemperature analysis.

SELECTING ARCHEAN CHERTS FOR PALEOTEMPERATURE ESTIMATES

We would emphasize that three conditions must be met for Archean cherts to be useful in surface paleotemperature analysis: (1) they should represent silica deposited under open marine conditions; (2) they should show no evidence for deposition or diagenesis involving meteoric or hydrothermal waters; and (3) the original siliceous

sediments should have undergone transformation to microquartz under surface or very shallow-burial conditions. We will discuss each of these criteria and its relevance to the samples analyzed here.

(1) Cherts used in paleotemperature analysis should represent sediments deposited in known depositional settings where a fluid or fluids of known or determinable composition controlled the sedimentation and early diagenesis. For Archean cherts, that fluid will most likely have been sea water because of the wide possible compositional variability of meteoric and hydrothermal waters. BGB cherts that are potentially useful for paleotemperature analysis include thick units of carbonaceous chert and banded chert in the BRC and at the top of the Mendon Formation. The origin of these and similar but thinner BGB chert units has been the subject of many investigations and presently there are two prevailing interpretations: (1) they represent hydrothermal or hydrothermally influenced silica deposits (de Wit and others, 1982; Paris and others, 1985; Westall and others, 2001, 2015; Hofmann, 2005; Hofmann and Bolhar, 2007; Hofmann and Harris, 2008) or (2) they formed largely from silica precipitated out of Archean sea water (Lowe and Knauth, 1977; Knauth and Lowe, 1978, 2003; Lowe, 1999; Stefurack and others, 2015a).

Sedimentological analysis of the black-and-white banded chert members of the BRC shows that they represent sediments deposited on a subsiding volcanic platform after volcanism had ceased regionally and after the volcanic edifice had been eroded down and subsided below sea level (Lowe, 1999; Tice and Lowe, 2006). The upward disappearance of siliciclastic debris eroded from the felsic complex marks the point where the complex was no longer subaerially exposed and yielded no debris or meteoric runoff because of the absence of subaerial exposures. The banded black and white cherts of the BRC represent biological and siliceous sediments deposited on this submerged and subsiding volcanic edifice after volcanic and thermal activity had ceased. Over much of the area, the BRC sea floor was within the photic zone (Tice and Lowe, 2004, 2006) and was a low-relief, overall low energy depositional surface covered widely by microbial mats and swept by weak currents that transported abundant carbonaceous particles. Occasional storms ripped up the partially lithified the sediments to form breccias and conglomerates (Lowe and Knauth, 1977; Lowe, 1999; Tice and Lowe, 2006; Knauth and Lowe, 1978, 2003). The properties of these deposits are most indicative of deposition through the accumulation of silica precipitated directly from sea water, much as fine to granular particulate sediments (Stefurack and others, 2015a; Ledevin, 2019).

(2) There is no evidence for deposition of the bulk of the BRC under the influence of hydrothermal fluids, meteoric waters, or mixed meteoric and marine waters. As noted above, cherts in the evaporitic member of the BRC show evidence for deposition in shallow brine ponds (Lowe and Fisher-Worrell, 1999). A sample of chert from these evaporites (SAF-135) shows a relatively low $\delta^{18}O$ value of 16.5‰ (table 1) that most likely reflects the influence of meteoric waters on sedimentation and diagenesis.

Interpretations of a hydrothermal origin for BGB cherts rest mainly on their geochemistry: trace element compositions often more resemble those of younger hydrothermal than modern marine fluids (Hofmann, 2005; Hofmann and Bolhor, 2007). However, we have found no features in the BRC and most other BGB cherts similar to those seen in siliceous deposits associated with and surrounding modern and ancient hydrothermal vents and an abundance of features most consistent with deposition of fine, well-layered sediments under open marine conditions, summarized above. It is key to note that the ultimate source of the silica may have included hydrothermal fluids but that by the time that sedimentation occurred, those fluids had mixed with and were indistinguishable from sea water. Most Phanerozoic subaqueous and subaerial hydrothermal near-vent deposits are lenticular accumulations of silica, carbonate, and

iron-rich sediments that thin rapidly away from the vents (for example, Snyder, 1978; Baross and Hoffman, 1985; Lowe and others, 2001). Subaerial siliceous sinter is dominated by microbial mats and shows abundant microbial structures (Jones and Renaut, 1996; Jones and others, 1997). Most also shows distinctive sedimentary structures related to silica deposition driven by rapid water cooling and, in the case of subaerial sinter, evaporation (Braunstein and Lowe, 2001; Lowe and Braunstein, 2003). Bed lenticularity, rapid lateral facies changes, and polymetallic mineralization (Snyder, 1978) are widespread, none of which characterize or are known from the Buck Reef Chert. The BRC is 250 to 400 m thick and outcrops continuously along strike for over 35 km in the southern BGB. It is a finely banded to laminated unit throughout that lacks lenticular build-ups or units that could be interpreted as siliceous sinter mounds or other deposits localized around hydrothermal vents, biotic or abiotic structures like those present in modern siliceous sinter deposits, and no evidence for cross-cutting hydrothermal conduits active during deposition, chimneys, degraded or otherwise, or similar irregular buildups or debris from such buildups that might mark vents. Both the BRC and upper Mendon cherts in the areas studied lack significant syndepositional metal enrichment and polymetallic mineral deposits common to younger hydrothermal accumulations (Snyder, 1978).

Hofmann (2005) suggests that the hydrothermal waters from which the cherts were deposited were very low-temperature waters that seeped upward through underlying rocks and sediments. Hofmann and Harris (2008), in a study of the formation of zones of silicification and alteration underlying many chert units, suggests that: "The element depletion-enrichment patterns and oxygen isotope data indicate low-temperature (*ca.* 100–150 °C) hydrothermal processes for the origin of the alteration zones. The loss of most elements coupled with the addition of SiO_2 as well as REE systematics indicate high water–rock ratios and a fluid REE composition typical of Archaean seawater that had a $\delta^{18}O$ value of ~0 permil." We would suggest that these low-temperature hydrothermal fluids inferred to have been active in the deposition of BGB cherts were, in fact, sea water at warm to hot surface or near surface temperatures. Until more direct evidence for syndepositional hydrothermal conduits, vents and near-vent deposits, sinter mounds, polymetallic mineralization, and other features characteristic of hydrothermal deposits in younger geologic time can be found in the BRC and related BGB cherts, we consider it most likely that these deposits represent normal Archean marine sediments.

We would also add that the extreme impermeability of the lithified Buck Reef Chert and similar thick chert units in the BGB makes it very unlikely that hydrothermal fluids could have widely percolated upward through these chert layers after more than a few meters had accumulated and lithified. The present samples would have been surrounded in all directions after deposition and early lithification by highly impermeable chert and would probably have not been open to interaction with ascending deeper-level hydrothermal fluids that had reacted extensively with underlying volcanic rocks, as characterizes many volcanic accumulations in the geologic record (Zakharov and others, 2019; Zakharov and Bindemen, 2019).

(3) Because the evolution of primary, possibly amorphous silica deposits to cherts composed of microquartz involves a series of diagenetic steps toward progressively more ordered forms of silica (for example, Williams and Crerar, 1985; Behl and Garrison, 1994; Yanchilina and others, 2019), it is possible that the final isotopic composition reflects the influence of deep burial waters and conditions substantially different from those that prevailing during silica deposition. The timing of the transformation of the original siliceous sediments to quartz and of later diagenesis affecting chert oxygen-isotopic signatures in the BGB was considered by Knauth and Lowe (2003). These authors performed 2 particularly relevant tests to establish when

the oxygen isotopic composition of these sediments was set and locked in: (i) analysis of the isotopic compositions of adjacent black and white chert bands in the BRC, and (ii) analysis of the isotopic compositions of pebbles in conglomerates in the Fig Tree and Moodies Groups.

(i) At least some of the white chert bands in the black and white banded cherts were deposited as soft, oozy to plastic sediment that exhibited soft-sediment deformation and foundering when deposited on interlayered, soft, low-density carbonaceous sediments (fig. 3B). However, the white chert layers were widely lithified early, as shown by the widespread chert plate breccias (fig. 6) formed by early rip-up of rigid or semi-rigid plates of white chert during storms and other wave and/or current events (Lowe and Knauth, 1977; Tice and Lowe, 2006). Lowe and Knauth (1977) and Knauth and Lowe (2003) suggest that most white bands were lithified within a meter or so of the sediment surface. Lowe and Knauth (1977, their fig. 16) show white-chert-plate breccias in which the brittle-fractured white chert plates were exposed at the sediment surface and draped by current-deposited sediments. The dark carbonaceous bands remained soft and viscous long after deposition, forming the matrix to most chert plate breccias and widely forming dikes of still soft, unlithified carbonaceous sediment injected into underlying rocks along fractures (Lowe and Knauth, 1977; Lowe, 2013).

Knauth and Lowe (2003) analyzed the $\delta^{18}O$ of adjacent black and white chert bands in the BRC. Of 10 black and white band pairs analyzed, the white chert bands in 9 had $\delta^{18}O$ greater (up to 1.6‰) than the adjacent black chert bands: in one band pair they were the same. These differences were interpreted to reflect the earlier formation of microquartz in the white bands at somewhat shallower depths and lower temperatures than the microquartz in the black bands, consistent with the relative timing of lithification as suggested by the band properties. Preservation of these subtle isotopic differences suggests that no subsequent long-term isotopic "drift", hydrothermal alteration, or late diagenesis or metamorphism has affected these rocks and reset and homogenized the slightly different oxygen-isotopic band compositions.

(ii) The $\delta^{18}O$ compositions of clasts of white and black chert in conglomerates in the stratigraphically higher Fig Tree and Moodies Groups were also analyzed by Knauth and Lowe (2003). If large-scale, long-term resetting of the BGB rocks has occurred, the isotopic composition of conglomerate clasts should have been homogenized. Chert pebbles in conglomerates show significant differences in $\delta^{18}O$ compositions, even within individual beds, indicating a lack of long-term isotopic homogenization. Comparison of Fig Tree and Moodies conglomerates also suggests that the clasts record progressive erosion down into the underlying Onverwacht Group. Knauth and Lowe (1978, 2003) showed that the Onverwacht Group can be divided into two major O-isotopic divisions. Below the ~3.445 Ga H6 felsic volcanic unit (fig. 1), which directly underlies the BRC, white bands in black-and-white banded cherts show relatively low $\delta^{18}O$ values, commonly +11 to +16‰ and many show a fine, sugary texture that is absent in most cherts above H6. They interpreted these low values to reflect flushing of the sequence below H6 by voluminous hydrothermal fluids, probably during regional metamorphic events associated with the eruption of ~3.445 Ga H6 volcanic rocks, emplacement of shallow hypabyssal intrusions in H6, and intrusion of deeper-level tonalite-trondhjemite-granodiorite (TTG) plutons of the Stolzberg TTG suite. Two of the samples analyzed in this study are from units of black and white banded chert below H6, samples SAF-52-8 and SAF-52-13, which show $\delta^{18}O$ of 14.4‰ and 15.4‰, respectively (table 1). Above H6, $\delta^{18}O$ of cherts in the Kromberg and Mendon Formations, including the BRC, are widely in the range of +17 to +21‰. Knauth and Lowe (2003) reported that 15 samples of cherts from the Mendon Formation had $\delta^{18}O$ from +18 to +22‰. Chert clasts in

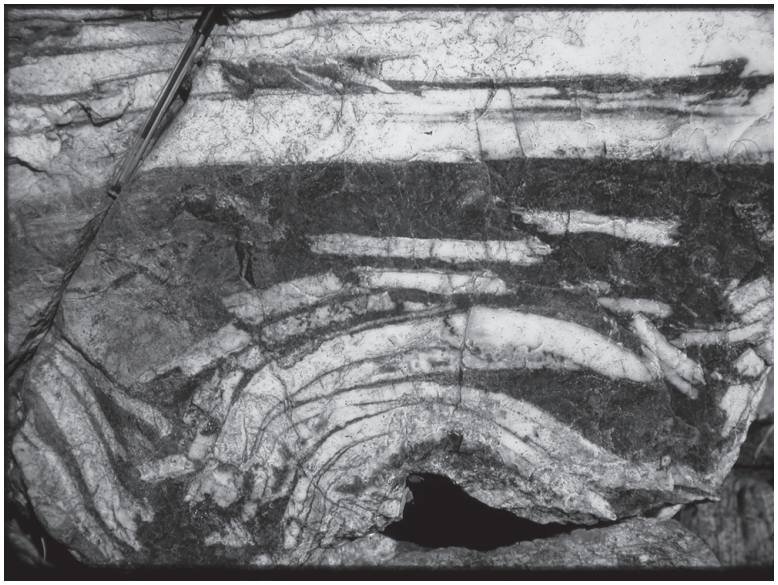

Fig. 6. Syn-sedimentary breccia in the Buck Reef Chert. The chert plates show brittle fracture and breakage of original white chert bands but later soft-sediment deformation to form a anticline-like fold of a stack of chert plates. The bands were deposited as a gel-like soft sediment that quickly hardened to form brittle layers. Pen (upper left) is 15 cm long.

middle Fig Tree conglomerates show $\delta^{18}O$ of +20 to +21.1‰, consistent with their derivation by erosion of cherts of the Mendon Formation. Stratigraphically higher Fig Tree conglomerate clasts showed $\delta^{18}O$ of +15.4 to +17‰ and Moodies conglomerates contained abundant clasts with $\delta^{18}O$ of +11.4 to +17‰. The upward change in conglomerate clast composition through the Fig Tree and Moodies Groups appears to reflect progressive uplift and deeper erosion into the Onverwacht Group. Lower and middle Fig Tree conglomerates reflect erosion of rocks above H6, younger than the 3.445 Ga event, and upper Fig Tree and Moodies conglomerates reflect erosion down into hydrothermally altered and recrystallized rocks below H6. These interpretations are also consistent with interpretations based on sandstone modal analysis and shale geochemistry that the Fig Tree Group was derived by erosion of the volcanic portion of the greenstone belt and the Moodies Group was sourced in large part from deeper-level TTG plutons (Heubeck and Lowe, 1999; Hessler and Lowe, 2006; Heubeck, 2019).

We therefore suggest that in the BRC, and probably other BGB cherts younger than Member H6 of the Hooggenoeg Formation, transformation of the original sediments to microquartz occurred at very shallow depths within a few meters of the sediment surface and under the influence of normal sea water and that burial diagenesis or alteration under the influence of hydrothermal or metamorphic fluids, which would have homogenized chert isotopic compositions, has not substantially altered the oxygen isotope values of the best preserved cherts.

CONCLUSIONS

The present study using triple oxygen analysis of 3.472 to 3.239 Ga cherts from the Early Archean Barberton Greenstone Belt, South Africa, has provided results, when viewed within the context of geologic setting and processes of deposition, suggesting that Archean surface temperatures were well above those of the present day, in the

range of 66° to 76 °C if Archean sea water had essentially the same isotopic composition as modern ice-free sea water and the highest $\delta'^{18}O$ oxygen isotope measurements are used. Isotopic studies throughout the BGB and in the Pilbara of Western Australia are converging toward maximum preserved $\delta^{18}O$ values for Archean cherts of about 23 to 24 permil. We interpret the results to indicate that the Early Archean Earth (pre-3.0 Ga) was hot, reinforcing earlier suggestions of high Early Archean surface temperatures (Knauth and Lowe, 1978, 2003; Lowe and Tice, 2007).

One of the key results of the present study is to emphasize the importance of carefully collecting samples for O-isotope analysis from areas of known geology and depositional environment. Many types of chert, such as deep-water cherts, nodular cherts, and most intertidal cherts, are unsuitable for estimating ancient surface paleotemperatures because their early diagenesis was likely influenced by fluids other than normal sea water. Group 2 samples in the present study all contain potentially useful isotopic information but were affected by problematic post-depositional processes, such as thermal effects of nearby diabase dikes and sills, regional metamorphism, or deposition in environments that were influenced by meteoric or evaporitic waters. These effects cannot be easily recognized in hand specimens: they need to be worked out in the field prior to sample collection and then verified through isotopic studies. Most museum specimens of Archean cherts, unless accompanied by systematic field and sedimentological information, are not useful for paleotemperature analysis. We would emphasize that simple grab sampling, even from core or where the outcropping rocks look fresh, can produce uninterpretable or incorrect results because of unrecognized depositional or post-depositional processes that have affected the rocks.

ACKNOWLEDGMENTS

We are grateful to the School of Earth, Energy, and Environmental Sciences at Stanford University, which provided partial funding to support this research; to the National Science Foundation, which funded key parts of the early stages of this research; the NASA Exobiology Program grants NCC-2-721, NAG5-98421, and NNG04GM43G to DRL; the Mpumalanga Tourism and Parks Agency, especially Mr. Johan Eksteen, and Sappi Forest Products, which allowed us access to private lands; and the many mining geologists and interested Barberton residents who have helped the authors in their studies throughout the years. CPC and DEI's development of triple oxygen isotope methods were supported by a grant to the Heising-Simons Foundation. We acknowledge Z. Sharp, J. Wostbrock, M. Lloyd, T. Kukla and D. Stolper for guidance and advice, and Paul Knauth for sharing his encyclopedic knowledge of stable isotopes and chert. DEI is supported by a UC President's Postdoctoral Fellowship and a Miller Institute Fellowship.

AUTHOR CONTRIBUTIONS

D.R.L. and D.E.I. contributed equally to this work. DRL designed the study in collaboration with all authors, conducted the field work, and assembled all samples, some of which had been collected by Michael Tice (Tice and Lowe, 2006). DEI and CPC made the measurements; DRL, DEI, and ND made the figures; and DRL wrote the paper with input from all authors.

APPENDIX

TABLE A1

Triple oxygen isotope data of samples from the Barberton Greenstone Belt, South Africa (3.47 to 3.25 Ga)

Sample ID	Sample Type	Formation	Age (Ga)	$\delta^{18}O$ (VSMOW)	$\delta'^{17}O$ (VSMOW)	$\delta'^{18}O$ (VSMOW)	SE	$\Delta'^{17}O$ (λ=0.528)	SE	No. of Anal.	Sample Group	Notes
Samples												
TSA5-5	White Chert	BRC, Kromberg Fm.	~3400	21.897	11.311	21.661	0.007	-0.126	0.008	3	1	High variability in $\delta'^{18}O$ and $\Delta^{17}O$
				19.722	10.283	19.530	0.003	-0.029	0.004			
				18.927	9.844	18.750	0.005	-0.056	0.006			
TSA5-7	White Chert	BRC, Kromberg Fm.	~3400	19.219	10.012	19.037	0.004	-0.040	0.004	2	1	
				17.716	9.233	17.561	0.011	-0.040	0.006			
TSA5-8	White Chert	BRC, Kromberg Fm.	~3400	18.658	9.662	18.486	0.006	-0.098	0.007	1		Low $\Delta^{17}O$ not included in groups 1 or 2
TSA5-10	White Chert	BRC, Kromberg Fm.	~3400	18.347	9.556	18.181	0.008	-0.043	0.008	3	1	High variability in $\Delta^{17}O$
				18.015	9.369	17.854	0.004	-0.058	0.007			
				18.093	9.434	17.931	0.004	-0.034	0.007			
TSA5-30	White Chert	BRC, Kromberg Fm.	~3400	19.964	10.399	19.767	0.007	-0.038	0.010	1	1	
TSA5-22	Black Chert	BRC, Kromberg Fm.	~3400	20.068	10.411	19.869	0.009	-0.080	0.009	1	1	
SAF-52-8	White Chert	lower Hooggenoeg Fm.	~3472	14.670	7.648	14.563	0.009	-0.041	0.007	1	2	
SAF-52-13	White Chert	lower Hooggenoeg Fm.	~3472	15.171	7.898	15.057	0.008	-0.052	0.007	1	2	
SAF-73-7	White Chert	Mapape Fm., Fig Tree Gr.	~3240	16.551	8.635	16.416	0.009	-0.032	0.008	4	1	High variability in $\delta'^{18}O$
				18.428	9.611	18.260	0.004	-0.030	0.008			
				16.654	8.690	16.517	0.005	-0.030	0.004			
				18.643	9.712	18.471	0.012	-0.041	0.008			
SAF-131-11	White Chert	BRC, Kromberg Fm.	~3400	19.720	10.243	19.528	0.006	-0.068	0.008	3	1	
				18.666	9.726	18.493	0.007	-0.039	0.009			
				19.466	10.110	19.279	0.004	-0.069	0.006			
SAF-131-12	White Chert	BRC, Kromberg Fm.	~3400	19.976	10.385	19.779	0.004	-0.059	0.007	1	1	
SAF-135-4	White Chert	upper Hooggenoeg Fm.	~3420	16.075	8.381	15.947	0.010	-0.039	0.008	1	2	
SAF-160-4	Black Chert	BRC, Kromberg Fm.	~3400	20.881	10.846	20.666	0.008	-0.065	0.007	1	1	
SAF-475-2	White Chert	BRC, Kromberg Fm.	~3400	15.992	8.341	15.865	0.002	-0.036	0.003	1	2	
Standards							**SD**		**SD**			**Standard Values**
NM-Q[1]	Quartz			18.147	9.410	17.985	0.137	-0.086	0.018	47		$\delta'^{18}O$ = 17.909; $\Delta'^{17}O$ = -0.081
SCO[2]	Olivine			5.501	2.835	5.486	0.587	-0.062	0.012	23		$\delta'^{18}O$ = 5.255; $\Delta'^{17}O$ = -0.058
UWG-2[3]	Garnet			5.622	2.896	5.606	0.611	-0.064	0.018	16		$\delta'^{18}O$ = 5.680; $\Delta'^{17}O$ = -0.071

SE (Standard Error) values are calculated only for standards and samples with replicates. SD (Standard Deviation) values for samples without replicates are assumed to be equivalent to the hydrothermal quartz standard NM-Q used to monitor daily and session variability. All measurements are calibrated following the pressure baseline correction of Yeung and others (2019) and reported relative to published values of $\delta'^{18}O$ and $\Delta'^{17}O$ values of NM-Q, SCO and UWG-2 run during each session (values from Pack and Herwartz, 2014; Sharp and others, 2016; Wostbrock and others, 2018, 2020; see Wostbrock and others (2020) for values). Measurements made from October 2018 to July 2019. Standards are included from sessions when samples presented here were measured.

REFERENCES

Allwood, A. C., Walter, M. R., Kamber, B. S., Marshall, C. P., and Burch, I. W., 2006, Stromatolite reef from the Early Archaean era of Australia: Nature, v. 441, n. 7094, p. 714–718, https://doi.org/10.1038/nature04764

Baross, J. A., and Hoffman, S. E., 1985, Submarine hydrothermal vents and associated gradient environments as sites for the origin and evolution of life: Origins of Life, v. 15, p. 327–345, https://doi.org/10.1007/BF01808177

Becker, R. H., and Clayton, R. N., 1976, Oxygen isotope study of a Precambrian banded iron formation, Hamersley Range, Western-Australia: Geochimica et Cosmochimica Acta, v. 40, n. 10, p. 1153–1165, https://doi.org/10.1016/0016-7037(76)90151-4

Behl, R. J., and Garrison, R. E., 1994, The origin of chert in the Monterey Formation of California (USA), *in* Iijima, A., and Garrison, R., editors, Siliceous, phosphatic and glauconitic sediments of the Tertiary and Mesozoic. Utrecht, The Netherlands, Proceedings of the 29th International Geological Congress Part C, VSP, p. 101–132.

Blake, R. E., Chang, S. E., and Lepland, A., 2010, Phosphate isotopic evidence for a temperate and biologically active Archaean ocean: Nature, v. 464, p. 1029–1032, https://doi.org/10.1038/nature08952

Braunstein, D., and Lowe, D. R., 2001, Relationship between spring and geyser activity and the deposition and morphology of high temperature (>73°C) siliceous sinter, Yellowstone National Park, Wyoming, USA: Journal of Sedimentary Research, v. 71, n. 5, p. 747–763, https://doi.org/10.1306/2DC40965-0E47-11D7-8643000102C1865D

Byerly, G. R., Kröner, A., Lowe, D. R., Todt, W., and Walsh, M. W., 1996, Prolonged magmatism and time constraints for sediment deposition in the early Archean Barberton greenstone belt: Evidence from the upper Onverwacht and Fig Tree Groups: Precambrian Research, v. 78, n. 1–3, p. 125–138, https://doi.org/10.1016/0301-9268(95)00073-9

Byerly, G. R., Lowe, D. R., Wooden, J. L., and Xie, X., 2002, An Archean impact layer from the Pilbara and Kaapvaal Craton: Science, v. 297, n. 5585, p. 1325–1327, https://doi.org/10.1126/science.1073934

Cammack, J. N., Spicuzza, M. J., Cavosie, A. J., Van Kranendonk, M. J., Hickman, A. H., Kozdon, R., Orland, I. J., Kitajima, K., and Valley, J. W., 2018, SIMS microanalysis of the Strelley Pool Formation cherts and the implications for the secular-temporal oxygen-isotope trend of cherts: Precambrian Research, v. 304, p. 125–139, https://doi.org/10.1016/j.precamres.2017.11.005

Dann, J. C., 2000, The 3.5 Ga Komati Formation, Barberton greenstone belt, South Africa, Part I: New mas and magmatic architecture: South African Journal of Geology, v. 103, n. 1, p. 47–68, https://doi.org/10.2113/103.1.47

de Wit, M. J., Hart, R., Martin, A., and Abbott, P., 1982, Archean abiogenic and probable biogenic structures associated with mineralized hydrothermal vent systems and regional metasomatism, with implications for greenstone belt studies: Economic Geology, v. 77, n. 8, p. 1783–1802, https://doi.org/10.2113/gsecongeo.77.8.1783

Degens, E. T, and Epstein, S., 1964, Oxygen and carbon isotope ratios in coexisting calcites and dolomites from recent and ancient sediments: Geochimica et Cosmochimica Acta, v. 28, n. 1, p. 23–44, https://doi.org/10.1016/0016-7037(64)90053-5

Drabon, N., Lowe, D. R., and Heubeck, C. E., 2019, Evolution of an Archean fan delta and its implications for the initiation of uplift and deformation in the Barberton greenstone belt, South Africa: Journal of Sedimentary Research, v. 89, n. 9, p. 849–874, https://doi.org/10.2110/jsr.2019.46

Drieberg, S. L., Hagemann, S. G., Huston, D. L., Landis, G., Ryan, C. G., Van Achterbergh, E., and Vennemann, T., 2013, The interplay of evolved seawater and magmatic-hydrothermal fluids in the 3.24 Ga Panorama volcanic-hosted massive sulfide hydrothermal system, North Pilbara Craton, Western Australia: Economic Geology, v. 108, n. 1, p. 79–110, https://doi.org/10.2113/econgeo.108.1.79

Galili, N., Shemesh, A., Yam, R., Brailovsky, I., Sela-Adler, M., Schuster, E. M., Collom, C., Bekker, A., Planavsky, N., Macdonald, F. A., Préat, A., Rudmin, M., Trela, W., Sturesson, U., Heikoop, J. M., Aurell, M., Ramajo, J., and Halevy, I., 2019, The geologic history of seawater oxygen isotopes from marine iron oxides: Science, v. 365, n. 6452, p. 469–473, https://doi.org/10.1126/science.aaw9247

Gamper, A., Heubeck, C., Demskec, D., and Hoehse, M., 2012, Composition and microfacies of Archean microbial mats (Moodies Group, *ca.* 3.22 Ga, South Africa), *in* Noffke, N., and Chafetz, H., editors, Microbial Mats in Siliciclastic Depositional Systems Through Time: Society of Sedimentary Geology Special Publication 101, p. 65–74, https://doi.org/10.2110/sepmsp.101.065

Hayles, J. A., Yeung, L. Y., Homann, M., Banerjee, A., Jiang, H., Shen, B., and Lee, C.T., 2019, Three billion year secular evolution of the triple oxygen isotope composition of marine chert: Earth and Planetary Science Letters, https://doi.org/10.31223/OSF.IO/N2P5Q

Hessler, A. M., and Lowe, D. R., 2006, Weathering and sediment generation in the Archean: An integrated study of the evolution of siliciclastic sedimentary rocks of the 3.2 Ga Moodies Group, Barberton Greenstone Belt, South Africa: Precambrian Research, v. 151, n. 3–4, p. 185–210, https://doi.org/10.1016/j.precamres.2006.08.008

Heubeck, C., 2009, An early ecosystem of Archean tidal microbial mats (Moodies Group, South Africa, *ca.* 3.2 Ga): Geology, v. 37, n. 10, p. 931–934, https://doi.org/10.1130/G30101A.1

_____ 2019, The Moodies Group - A high-resolution archive of Archaean surface processes and basin-forming processes, *in* Kröner, A., and Hofmann, A., editors, The Archaean Geology of the Kaapvaal Craton, southern Africa: Regional Geology Reviews, v. 133, p. 133–169, https://doi.org/10.1007/978-3-319-78652-0_6

Heubeck, C., and Lowe, D. R., 1999, Sedimentary petrography and provenance of the Archean Moodies Group, Barberton Greenstone Belt, *in* Lowe, D. R., and Byerly, G. R., editors, Geologic evolution of

the Barberton Greenstone Belt, South Africa: GSA Special Paper 329, p. 259–286, https://doi.org/10.1130/0-8137-2329-9.259

Heubeck, C., Engelhardt, J., Byerly, G. R., Zeh, A., Sell, B., Luber, T., and Lowe, D. R., 2013, Timing of deposition and deformation of the Moodies Group (Barberton Greenstone belt, South Africa): Very-high-resolution of Archaean surface processes: Precambrian Research, v. 231, p. 236–262, https://doi.org/10.1016/j.precamres.2013.03.021

Hofmann, A., 2005, The geochemistry of sedimentary rocks from the Fig Tree Group, Barberton Greenstone Belt: Implications for tectonic, hydrothermal and surface processes during mid-Archean times: Precambrian Research, v. 143, n. 1–4, p. 23–49, https://doi.org/10.1016/j.precamres.2005.09.005

Hofmann, A., and Bolhar, R., 2007, Carbonaceous cherts in the Barberton Greenstone Belt and their significance for the study of early life in the Archean record: Astrobiology, v. 7, n. 2, p. 355–388, https://doi.org/10.1089/ast.2005.0288

Hofmann, A., and Harris, C., 2008, Silica alteration zones in the Barberton greenstone belt: a window into subseafloor processes 3.5-3.3 Ga ago: Chemical Geology, v. 257, n. 1–4, p. 221–239, https://doi.org/10.1016/j.chemgeo.2008.09.015

Homann, M., Heubeck, C., Airo, A., and Tice, M. M., 2015, Morphological adaptations of 3.22 Ga-old tufted microbial mats to Archean coastal habitats (Moodies Group, Barberton Greenstone Belt, South Africa): Precambrian Research, v. 266, p. 47–64, https://doi.org/10.1016/j.precamres.2015.04.018

Hren, M. T., Tice, M. M., and Chamberlain, C. P., 2009, Oxygen and hydrogen isotope evidence for a temperate climate 3.42 billion years ago: Nature, v. 462, p. 205–208, https://doi.org/10.1038/nature08518

Jaffrés, J. B. D., Shields, G. A., and Wallmann, K., 2007, The oxygen isotope evolution of seawater: A critical review of a long-standing controversy and an improved geological water cycle model for the past 3.4 billion years: Earth-Science Reviews, v. 83, n. 1–2, p. 83–122, https://doi.org/10.1016/j.earscirev.2007.04.002

Johnson, B. W., and Wing, B. A., 2020, Limited Archaean continental emergence reflected in an early Archaean ^{18}O-enriched ocean: Nature Geoscience, v. 13, p. 243–248, https://doi.org/10.1038/s41561-020-0538-9

Jones, B., and Renaut, R. W., 1996, Influence of thermophilic bacteria on calcite and silica precipitation in hot springs with water temperatures above 90°C: Evidence from Kenya and New Zealand: Canadian Journal of Earth Sciences, v. 33, p. 72–83, https://doi.org/10.1139/e96-008

Jones, B., Renaut, R. W., and Rosen, M. R., 1997, Biogenicity of silica precipitation around geysers and hot-spring vents, North Island, New Zealand: Journal of Sedimentary Research, v. 67, n. 1, p. 88–104, https://doi.org/10.1306/D42684FF-2B26-11D7-8648000102C1865D

Kasting, J. F., Howard, M. T., Wallmann, K., Veizer, J., Shields, G., and Jaffres, J. B. D., 2006, Paleoclimates, ocean depth, and the oxygen isotopic composition of seawater: Earth and Planetary Science Letters, v. 252, n. 1–2, p. 82–93, https://doi.org/10.1016/j.epsl.2006.09.029

Katrinak, K. A., ms, 1987, Stable isotope studies of cherts from the Archean Swaziland Supergroup of South Africa: Phoenix, Arizona, Arizona State University, MS thesis, 100 p.

Kerrich, R., and Fryer, B. J., 1979, Archaean precious-metal hydrothermal systems, Dome Mine, Abitibi Greenstone Belt. II. REE and oxygen isotope relations: Canadian Journal of Earth Sciences, v. 16, p. 440–458, https://doi.org/10.1139/e79-041

Knauth, L. P., ms, 1973, Oxygen and hydrogen isotope ratios in cherts and related rocks: Pasadena, California, California Institute of Technology, Ph. D. Thesis, 369 p.

_____1979, A model for the origin of chert in limestone: Geology, v. 7, n. 6, p. 274–277, https://doi.org/10.1130/0091-7613(1979)7<274:AMFTOO>2.0.CO;2

_____1992, Origin and diagenesis of cherts: An isotopic perspective in isotopic signatures and sedimentary records, *in* Clauer, N., and Chaudhuri, S., editors, Lecture Notes in Earth Sciences #43: Switzerland, Springer-Verlag, p. 123–152.

Knauth, L. P., and Epstein, S., 1976, Hydrogen and oxygen isotope ratios in nodular and bedded cherts: Geochimica et Cosmochimica Acta, v. 40, n. 9, p. 1095–1108, https://doi.org/10.1016/0016-7037(76)90051-X

Knauth, L. P., and Lowe, D.R., 1978, Oxygen isotope geochemistry of cherts from the Onverwacht Group (3.4 billion years), Transvaal, South Africa with implications for secular variations in the isotopic compositions of cherts: Earth and Planetary Science Letters, v. 41, n. 2, p. 209–222, https://doi.org/10.1016/0012-821X(78)90011-0

_____ 2003, High Archean climatic temperature inferred from oxygen isotope geochemistry of cherts in the 3.5 Ga Swaziland Supergroup, South Africa: GSA Bulletin, v. 115, n. 5, p. 566–580, https://doi.org/10.1130/0016-7606(2003)115<0566:HACTIF>2.0.CO;2

Kolodny, Y., and Epstein, S., 1976, Stable isotope geochemistry of deep sea cherts: Geochimica et Cosmochimica Acta, v. 40, n. 10, p. 1195–1209, https://doi.org/10.1016/0016-7037(76)90155-1

Kröner, A., Byerly, G. R., and Lowe, D. R., 1991, Chronology of early Archaean granite-greenstone evolution in the Barberton Mountain Land, South Africa, based on precise dating by single zircon evaporation: Earth and Planetary Science Letters, v. 103, n. 1–4, p. 41–54, https://doi.org/10.1016/0012-821X(91)90148-B

Kröner, A., Hegner, E., Wendt, J. I., and Byerly, G. R., 1996, The oldest part of the Barberton granitoid-greenstone terrain, South Africa: Evidence for crust formation between 3.5 and 3.7 Ga: Precambrian Research, v. 78, n. 1–3, p. 105–124, https://doi.org/10.1016/0301-9268(95)00072-0

Ledevin, M., 2019, Archean cherts: Formation processes and paleoenvironments, *in* Van Kranendonk, M. J., Bennett, V. C., and Hoffmann, J. E., editors, Earth's Oldest Rocks: Amsterdam, Elsevier, p. 913–944, https://doi.org/10.1016/B978-0-444-63901-1.00037-X

Levin, N. E., Raub, T. D., Dauphas, N., and Eiler, J. M., 2014, Triple oxygen isotope variations in sedimentary rocks: Geochimica et Cosmochimica Acta, v. 139, p. 173–189, https://doi.org/10.1016/j.gca.2014.04.034

Liljestrand, F. L., ms, 2019, The application of silica Δ'17O and δ18O towards paleo-environmental reconstructions: Cambridge, Massachusetts, Harvard University, Ph. D. dissertation, 189 p.

Liljestrand, F. L., Knoll, A. H., Tosca, N. J., Cohen, P. A., Macdonald, F. A., Peng, Y., and Johnston, D. T., 2020, The triple oxygen isotope composition of Precambrian chert: Earth and Planetary Science Letters, v. 537, https://doi.org/10.1016/j.epsl.2020.116167

Lowe, D. R., 1983, Restricted shallow-water sedimentation of early Archean stromatolitic and evaporitic strata of the Strelley Pool Chert, Pilbara Block, Western Australia: Precambrian Research, v. 19, n. 3, p. 239–283, https://doi.org/10.1016/0301-9268(83)90016-5

_____1999, Petrology and sedimentology of cherts and related silicified sedimentary rocks in the Swaziland Supergroup, *in* Lowe, D. R., and Byerly, G. R., editors, Geologic evolution of the Barberton Greenstone Belt, South Africa: GSA Special Paper 329, p. 83–114, https://doi.org/10.1130/0-8137-2329-9.83

_____2013, Crustal fracturing and chert dike formation triggered by large meteorite impacts, *ca.* 3.260 Ga, Barberton greenstone belt, South Africa: GSA Bulletin, v. 125, p. 894–912, https://doi.org/10.1130/B30782.1

Lowe, D. R., and Braunstein, D., 2003, Microstructure of high-temperature (>73°C) siliceous sinter deposited around hot springs and geysers, Yellowstone National Park: The role of biological and abiological processes in sedimentation: Canadian Journal of Earth Sciences, v. 40, n. 11, p. 1611–1642, https://doi.org/10.1139/e03-066

Lowe, D. R., and Byerly, G. R., 1999, Stratigraphy of the west-central part of the Barberton Greenstone Belt, South Africa, *in* Lowe, D. R., and Byerly, G. R., editors, Geologic Evolution of the Barberton Greenstone Belt, South Africa: GSA Special Paper 329, p. 1–36, https://doi.org/10.1130/0-8137-2329-9.1

Lowe, D. R., and Byerly, G. R., 2007, Ironstone bodies of the Barberton greenstone belt, South Africa: Products of a Cenozoic hydrological system, not Archean hydrothermal vents!: GSA Bulletin, v. 119, p. 65–87, https://doi.org/10.1130/B25997.1

Lowe, D. R., and Fisher-Worrell, G., 1999, Sedimentology, mineralogy, and implications of silicified evaporites in the Kromberg Formation, Barberton Greenstone Belt, South Africa, *in* Lowe, D. R., and Byerly, G. R., editors, Geologic evolution of the Barberton Greenstone Belt, South Africa: GSA Special Paper 329, p. 167–188, https://doi.org/10.1130/0-8137-2329-9.167

Lowe, D. R., and Knauth, L. P., 1977, Sedimentology of the Onverwacht Group (3.4 billion years), Transvaal, South Africa, and its bearing on the characteristics and evolution of the early earth: The Journal of Geology, v. 85, n. 6, p. 699–723, https://doi.org/10.1086/628358

Lowe, D. R., and Nocita, B. W, 1999, Foreland basin sedimentation in the Mapepe Formation, southern-facies Fig Tree Group, *in* Lowe, D. R., and Byerly, G.R., editors, Geologic Evolution of the Barberton Greenstone Belt, South Africa: GSA Special Paper 329, p. 233–258, https://doi.org/10.1130/0-8137-2329-9.233

Lowe, D. R., and Tice, M. M., 2007, Tectonic controls on atmospheric, climatic, and biological evolution 3.5–2.4 Ga: Precambrian Research, v. 158, n. 3–4, p. 177–197, https://doi.org/10.1016/j.precamres.2007.04.008

Lowe, D. R., Anderson, K. S., and Braunstein, D., 2001, The zonation and structuring of siliceous sinter around hot springs, Yellowstone National Park, and the role of thermophilic bacteria in its deposition, *in* Reysenbach, Voytek, M., and Mancinelli, R., editors, Thermophiles: Biodiversity, Ecology, and Evolution: New York, Kluwer Academic/Plenum, p. 143–166, https://doi.org/10.1007/978-1-4615-1197-7_11

Lowe, D. R., Byerly, G. R., and Heubeck, C., 2012, Geologic Map of the West-Central Barberton Greenstone belt, South Africa: Geological Society of America Map and Chart Series MCS103.

Marin, J., Chaussidon, M., and Robert, F., 2010, Microscale oxygen isotope variations in 1.9 Ga Gunflint cherts: Assessments of diagenesis effects and implications for oceanic paleotemperature reconstructions: Geochimica et Cosmochimica Acta, v. 74, n. 1, p. 116–130, https://doi.org/10.1016/j.gca.2009.09.016

Marin-Carbonne, J., Chaussidon, M., Boiron, M. -C., and Robert, F., 2011, A combined *in situ* oxygen, silicon isotopic and fluid inclusion study of a chert sample from Onverwacht Group (3.35 Ga, South Africa): New constraints on fluid circulation: Chemical Geology, v. 286, n. 3–4, p. 59–71, https://doi.org/10.1016/j.chemgeo.2011.02.025

Marin-Carbonne, J., Chaussidon, M., and Robert, F., 2012, Micrometer-scale chemical and isotopic criteria (O and Si) on the origin and history of Precambrian cherts: Implications for paleo-temperature reconstructions: Geochimica et Cosmochimica Acta, v. 92, p. 129–147, https://doi.org/10.1016/j.gca.2012.05.040

McBride, E. F., Abdel-Wahab, A., and El-Younsy, A. R. M., 1999, Origin of spheroidal chert nodules, Drunka Formation (Lower Eocene), Egypt: Sedimentology, v. 46, n. 4, p. 733–755, https://doi.org/10.1046/j.1365-3091.1999.00253.x

Mix, H. T., Ibarra, D. E., Mulch, A., Graham, S. A., and Chamberlain, C. P., 2016, A hot and high Eocene Sierra Nevada: GSA Bulletin, v. 128, n. 3–4, p. 531–542, https://doi.org/10.1130/B31294.1

Muehlenbachs, K., 1998, The oxygen isotopic composition of the oceans, sediments and the seafloor: Chemical Geology, v. 145, n. 3–4, p. 263–273, https://doi.org/10.1016/S0009-2541(97)00147-2

Muehlenbachs, K., and Clayton, R.N., 1976, Oxygen isotope composition of the oceanic crust and its bearing on seawater: Journal of Geophysical Research, v. 81, n. 23, p. 4365–4369, https://doi.org/10.1029/JB081i023p04365

Pack, A., and Herwartz, D., 2014, The triple oxygen isotope composition of the Earth mantle and understanding $\Delta^{17}O$ variations in terrestrial rocks and minerals: Earth and Planetary Science Letters, v. 390, p. 138–145, https://doi.org/10.1016/j.epsl.2014.01.017

Paris, I., Stanistreet, I. G., and Hughes, M. J., 1985, Cherts of the Barberton greenstone belt as products of submarine exhalative activity: The Journal of Geology, v. 93, n. 2, p. 111–129, https://doi.org/10.1086/628935

Perry Jr., E. C., 1967, The oxygen isotope chemistry of ancient cherts: Earth and Planetary Science Letters, v. 3, p. 62–66, https://doi.org/10.1016/0012-821X(67)90012-X

Perry Jr., E. C., and Tan, F. C., 1972, Significance of oxygen and carbon isotopic variations in early Precambrian cherts and carbonate rocks of South Africa: GSA Bulletin, v. 83, n. 3, p. 647–664, https://doi.org/10.1130/0016-7606(1972)83[647:SOOACI]2.0.CO;2

Perry Jr., E. C., Ahmad, S. N., and Swulius, T. M., 1978, The oxygen isotope composition of 3,800 m.y. old metamorphosed chert and iron formation from Isukasia, West Greenland: The Journal of Geology, v. 86, n. 2, p. 223–239, https://doi.org/10.1086/649676

Peters, S. T. M., Szilas, K., Sengupta, S., Kirkland, C. L., Garbe-Schönberg, D., and Pack, A., 2020, > 2.7 Ga metamorphic peridotites from southeast Greenland record the oxygen isotope composition of Archean seawater: Earth and Planetary Science Letters, v. 544, 116331, p. 13, https://doi.org/10.1016/j.epsl.2020.116331

Sengupta, S., and Pack, A., 2018, Triple oxygen isotope mass balance for the Earth's oceans with application to Archean cherts: Chemical Geology, v. 495, p. 18–26, https://doi.org/10.1016/j.chemgeo.2018.07.012

Sengupta, S., Peters, S. T. M., Reitner, J., Duda, J.-P., and Pack, A., 2020, Triple oxygen isotopes of cherts through time: Chemical Geology, v. 554, 119789, https://doi.org/10.1016/j.chemgeo.2020.119789

Sharp, Z. D., 1990, A laser-based microanalytical method for the *in situ* determination of oxygen isotope ratios of silicates and oxides: Geochimica et Cosmochimica Acta, v. 54, n. 5, p. 1353–1357, https://doi.org/10.1016/0016-7037(90)90160-M

Sharp, Z. D., Gibbons, J. A., Maltsev, O., Atudorei, V., Pack, A., Sengupta, S., Shock, E. L., and Knauth, L. P., 2016, A calibration of the triple oxygen isotope fractionation in the SiO_2-H2O system and applications to natural samples: Geochimica et Cosmochimica Acta, v. 186, p. 105–119, https://doi.org/10.1016/j.gca.2016.04.047

Sharp, Z. D., Wostbrock, J. A. G., and Pack, A., 2018, Mass-dependent triple oxygen isotope variations in terrestrial materials: Geochemical Perspective Letters, v. 7, p. 27–31, https://doi.org/10.7185/geochemlet.1815

Sleep, N. H., and Hessler, A. M., 2006, Weathering of quartz as an Archean climatic indicator: Earth and Planetary Science Letters, v. 241, n. 3–4, p. 594–602, https://doi.org/10.1016/j.epsl.2005.11.020

Sleep, N. H., and Zahnle, K., 2001, Carbon dioxide cycling and implications for climate on ancient Earth: Journal of Geophysical Research-Planets, v. 106, n. E1, p. 1373–1399, https://doi.org/10.1029/2000JE001247

Snyder, W. S., 1978, Manganese deposited by submarine hot springs in chert-greenstone complexes, western United States: Geology, v. 6, n. 12, p. 741–745, https://doi.org/10.1130/0091-7613(1978)6<741:MDBSHS>2.0.CO;2

Stefurak, E. J. T., Lowe, D. R., Zentner, D., and Fischer, W. W., 2015a, Sedimentology and geochemistry of Archean siica granules: GSA Bulletin, v. 127, n. 7–8, p. 1090–1107, https://doi.org/10.1130/B31181.1

Stefurak, E. J. T., Fischer, W. W., and Lowe, D. R., 2015b, Texture-specific Si isotope variations in Barberton Greenstone Belt cherts record low temperature fractionations in early Archean seawater: Geochemica et Cosmochimica Acta, v. 150, p. 26–52, https://doi.org/10.1016/j.gca.2014.11.014

Tartese, R., Chaussidon, A., Gurenko, A., Delarue, F., and Robert, F., 2017, Warm Archean oceans reconstructed from oxygen isotope composition of early-life remnants: Geochemical Perspective Letters, v. 3, n. 1, p. 55–65, https://doi.org/10.7185/geochemlet.1706

Tice, M. M., ms, 2005, Life and evolution in the early Archean - New data from the 3416 Ma Buck Reef Chert, Barberton Greenstone Belt, South Africa: Stanford, California, Stanford University, Ph. D. Dissertation, 122 p.

Tice, M. M., and Lowe, D. R., 2004, Photosynthetic microbial mats in the 3,416-Myr-old ocean: Nature, v. 431, p. 549–552, https://doi.org/10.1038/nature02888

_____2006, The origin of carbonaceous matter in pre-3.0 Ga greenstone terrains: A review and new evidence from the 3.42 Ga Buck Reef Chert: Earth Science Reviews, v. 76, n. 3–4, p. 259–300, https://doi.org/10.1016/j.earscirev.2006.03.003

Tice, M. M., Bostick, B. C., and Lowe, D. R., 2004, Thermal history of the 3.5–3.2 Ga Onverwacht and Fig Tree Groups, Barberton Greenstone Belt, South Africa: Geology, v. 32, n. 1, p. 37–40, https://doi.org/10.1130/G19915.1

Valley, J. W., Kitchen, N., Kohn, M. J., Niendorf, C. R., and Spicuzza, M. J., 1995, UWG-2, a garnet standard for oxygen isotope ratios: Strategies for high precision and accuracy with laser heating: Geochimica et Cosmochimica Acta, v. 59, n. 24, p. 5223–5231, https://doi.org/10.1016/0016-7037(95)00386-X

Yanchilina, A. G., Yam, R., Kolodny, Y., and Shemesh, A., 2019, From diatom opal-A $\delta^{18}O$ to chert $\delta^{18}O$ in deep sea sediments: Geochemica et Cosmochemica Acta, v. 268, p. 368–382, https://doi.org/10.1016/j.gca.2019.10.018

Verard, C., and Veizer, J., 2019, On plate tectonics and ocean temperatures: Geology, v. 47, n. 9, p. 881–885, https://doi.org/10.1130/G46376.1

Viljoen, M. J., and Viljoen, R. P., 1969, The geological and geochemical significance of the upper formations of the Onverwacht Group: Geological Society of South Africa Special Publication 2, p. 55–85.

Wallman, K., 2001, The geological water cycle and the evolution of $\delta^{18}O$ values: Geochimica et Cosmochimica Acta, v. 65, n. 15, p. 2469–2485, https://doi.org/10.1016/S0016-7037(01)00603-2

Westall, F., de Wit, M. J., Dann, J., van der Gaast, S., de Ronde, C. E. J., and Gerneke, D., 2001, Early Archean fossil bacteria and biofilms in hydrothermally-influenced sediments from the Barberton Greenstone Belt, South Africa: Precambrian Research, v. 106, n. 1–2, p. 93–116, https://doi.org/10.1016/S0301-9268(00)00127-3

Westall, F., Campbell, K. A., Bréhéret, J. G., Foucher, F., Gautret, P., Hubert, A., Sorieul, S., Grassineau, N., and Guido, D. M., 2015, Archean (3.33 Ga) microbe-sediment systems were diverse and flourished in a hydrothermal context: Geology, v.43, n. 7, p. 615–618, https://doi.org/10.1130/G36646.1

Williams, L. A., and Crerar, D. A., 1985, Silica diagenesis, II. General mechanisms: Journal of Sedimentary Petrology, v. 55, n. 3, p. 312–321, https://doi.org/10.1306/212F86B1-2B24-11D7-8648000102C1865D

Wostbrock, J. A. G., Sharp, Z. D., Sanchez-Yanez, C., Reich, M., van den Heuvel, D. B., and Benning, L. G., 2018, Calibration and application of silica-water triple oxygen isotope thermometry to geothermal systems in Iceland and Chile: Geochimica et Cosmochimica Acta, v. 234, p. 84–97, https://doi.org/10.1016/j.gca.2018.05.007

Wostbrock, J. A. G., Cano, E. J., and Sharp, Z. D., 2020, An internally consistent triple oxygen isotope calibration of standards for silicates, carbonates and air relative to VSMOW2 and SLAP2: Chemical Geology, v. 533, article number 119432, https://doi.org/10.1016/j.chemgeo.2019.119432

Xie, X., Byerly, G. R., and Ferrell Jr., R. E., 1997, IIb trioctahedral chlorite from the Barberton Greenstone Belt: Crystal structure and rock composition constraints with implications to geothermometry: Contributions to Mineralogy and Petrology, v. 126, p. 275–291, https://doi.org/10.1007/s004100050250

Yapp, C., 2001, Rusty relics of earth history: Iron (III) oxides, isotopes, and surficial environments: Annual Review of Earth and Planetary Sciences, v. 29, p. 165–199, https://doi.org/10.1146/annurev.earth.29.1.165

Yeung, L. Y., Hayles, J. A., Hu, H., Ash, J. L., and Sun, T., 2018, Scale distortion from pressure baselines as a source of inaccuracy in triple-isotope measurements: Rapid Communications in Mass Spectrometry, v. 32, n. 20, p. 1811–1821, https://doi.org/10.1002/rcm.8247

Zakharov, D. O., and Bindeman, I. N., 2019, Triple oxygen and hydrogen isotopic study of hydrothermally altered rocks from the 2.43–2.41 Ga Vetreny belt, Russia: An insight into the early Paleoproterozoic seawater: Geochimica et Cosmochimica Acta, v.248, p. 185–209, https://doi.org/10.1016/j.gca.2019.01.014

Zakharov, D. O., Bindeman, I. N., Tanaka, R., Friðleifsson, G. Ó., Reed, M. H., and Hampton, R. L., 2019, Triple oxygen isotope systematics as a tracer of fluids in the crust: A study from modern geothermal systems of Iceland: Chemical Geology, v. 530, 119312, https://doi.org/10.1016/j.chemgeo.2019.119312